ELECTRONIC SUPPLEMENTARY INFORMATION

for the manuscript

Removal of Lead, Cadmium, and Aluminum Sulfate from Simulated and Real Water with Native and Oxidized Starches

Konstantin B. L. Borchert [1,†], Rahma Boughanmi [1,†], Berthold Reis [1], Philipp Zimmermann [1], Christine Steinbach [1], Peter Graichen [1], Anastasiya Svirepa [2], Johannes Schwarz [2], Regine Boldt [1], Simona Schwarz [1], Michael Mertig [2,3] and Dana Schwarz [1,*]

[1] Leibniz-Institut für Polymerforschung Dresden e.V., Hohe Str. 6, 01069 Dresden, Germany; borchert@ipfdd.de (K.B.L.B.); boughanmi@ipfdd.de (R.B.); reis@ipfdd.de (B.R.); zimmermann-philipp@ipfdd.de (P.Z.); steinbach@ipfdd.de (C.S.); graichen@ipfdd.de (P.G.); boldt@ipfdd.de (R.B.); simsch@ipfdd.de (S.S.)

[2] Kurt-Schwabe-Institut für Mess-und Sensortechnik Meinsberg e.V., Kurt-Schwabe-Str. 4, 04736 Waldheim, Germany; anastasiya.svirepa@ksi-meinsberg.de (A.S.); johannes.schwarz@ksi-meinsberg.de (J.S.); michael.mertig@tu-dresden.de (M.M.)

[3] Institute of Physical Chemistry, Technische Universität Dresden, 01062 Dresden, Germany

* Correspondence: schwarz-dana@ipfdd.de; Tel.: +49-351-46-58-542

† These authors contributed equally to this work.

Abstract: The separation of toxic pollutants like Pb^{2+}, Cd^{2+} and Al^{3+} from water is a constant challenge as contamination of natural water bodies is increasing. Al^{3+} and especially Pb^{2+} and Cd^{2+} are ecotoxic and highly toxic for humans even in ppb concentrations, therefore removal below a dangerous level is demanding. Herein, the potential adsorber material starch as it is ecofriendly, cheap and abundantly available was investigated. Thus, four different native starch samples (potato, corn, waxy corn and wheat starch) and two oxidized starches (oxidized potato and corn starch) were comprehensively analyzed with streaming potential and charge density measurements, SEM-EDX, ATR-FTIR, ^{1}H-NMR and TGA. Subsequently, the starch samples were tested for the adsorption of Pb^{2+}, Cd^{2+} and Al^{3+} from the respective sulfate salt solution. The adsorption process was analyzed by ICP-OES and SEM-EDX and the adsorption isotherms were fitted comparing Langmuir, Sips, and Dubinin-Radushkevich models. Oxidized starch, which chemical modification is one of the simplest, and also native potato starch were excellent natural adsorber materials for Al^{3+}, Cd^{2+} and especially Pb^{2+} in the low concentration range, exhibiting maximum adsorption capacities of 84 µmol/g, 71 µmol/g, and 104 µmol/g for oxidized potato starch, respectively.

Table of Content

1. Results

1.1 Characterization of the Starch Samples

1.1.1 ^{1}H-NMR Spectroscopy

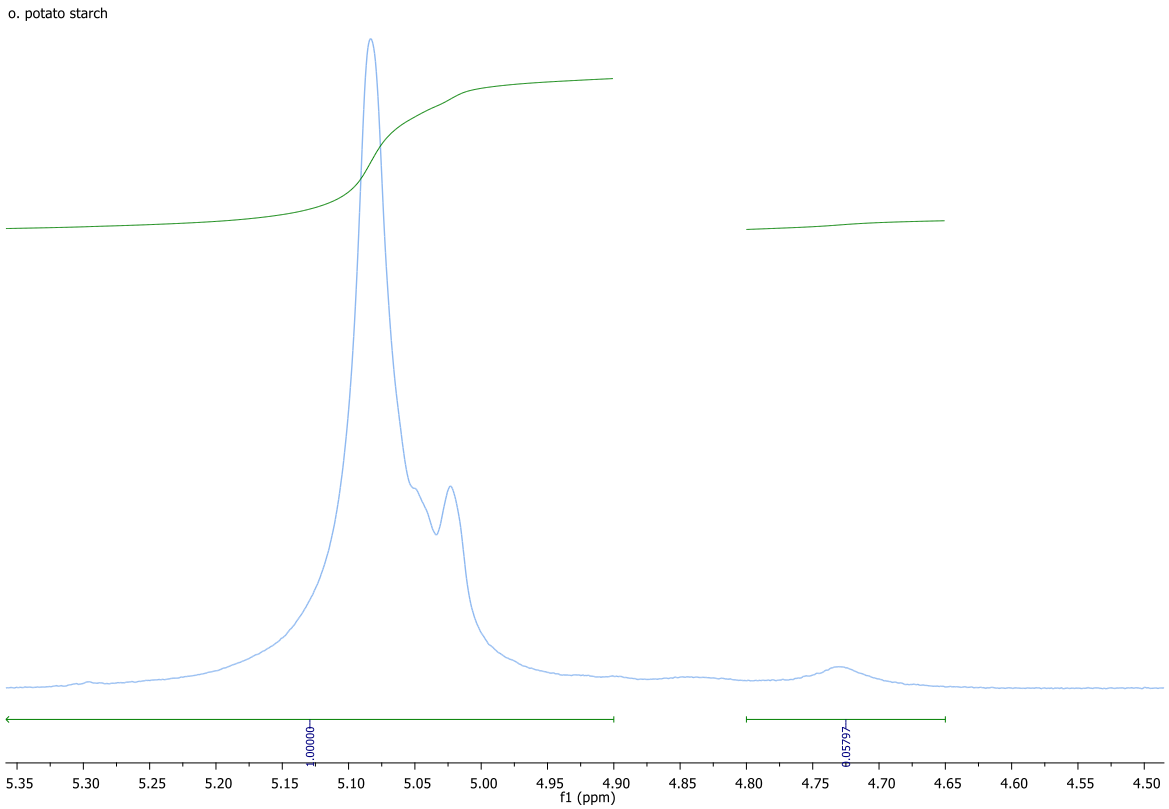

Figure S1. Integrals of H1 (α 1,4) + H1 (t) and H1 (α 1,6) from oxidized potato starch.

1.1.2 ATR-FTIR Spectroscopy

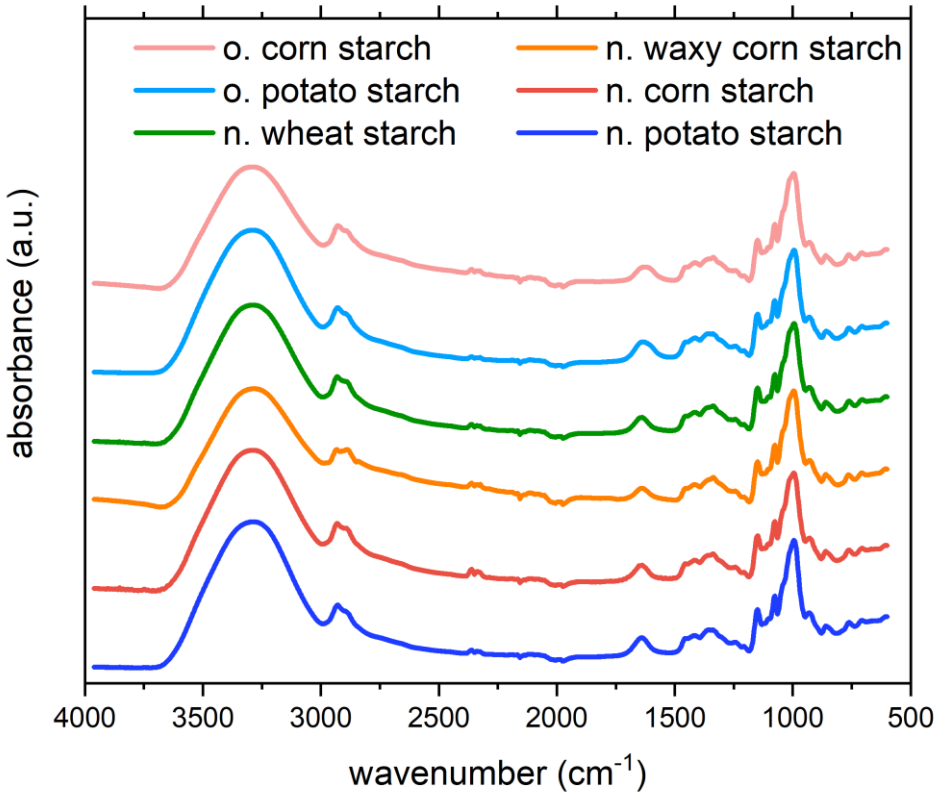

Figure S2. ATR-FTIR spectra of the solid native potato starch (blue), native corn starch (red), native waxy corn starch (orange), native wheat starch (green), oxidized potato starch (light blue) and oxidized corn starch (pink).

Table S1. FTIR vibration modes [1–3] for the starch samples.

Wavenumber (cm⁻¹)	**Vibration Mode**
3000–3680	O-H stretching
2933	CH2νas
2894	CH2νs
1643	water adsorbed in amorphous regions of starch
1457	CH2 δ
1418	CH bending
1371	CH δ
1336	COH bending/ deformation
1245	COH and CH bending of ring H
1150	C-O, C-C stretching
1079	C-O-H bending
998	CH2 related mode
930	C-O-C skeletal mode vibrations, related to α-1,4 glycosidic bond
858	C-O-H bending
765 + 706	C-C stretching

1.1.2 Moisture Analysis of the Samples

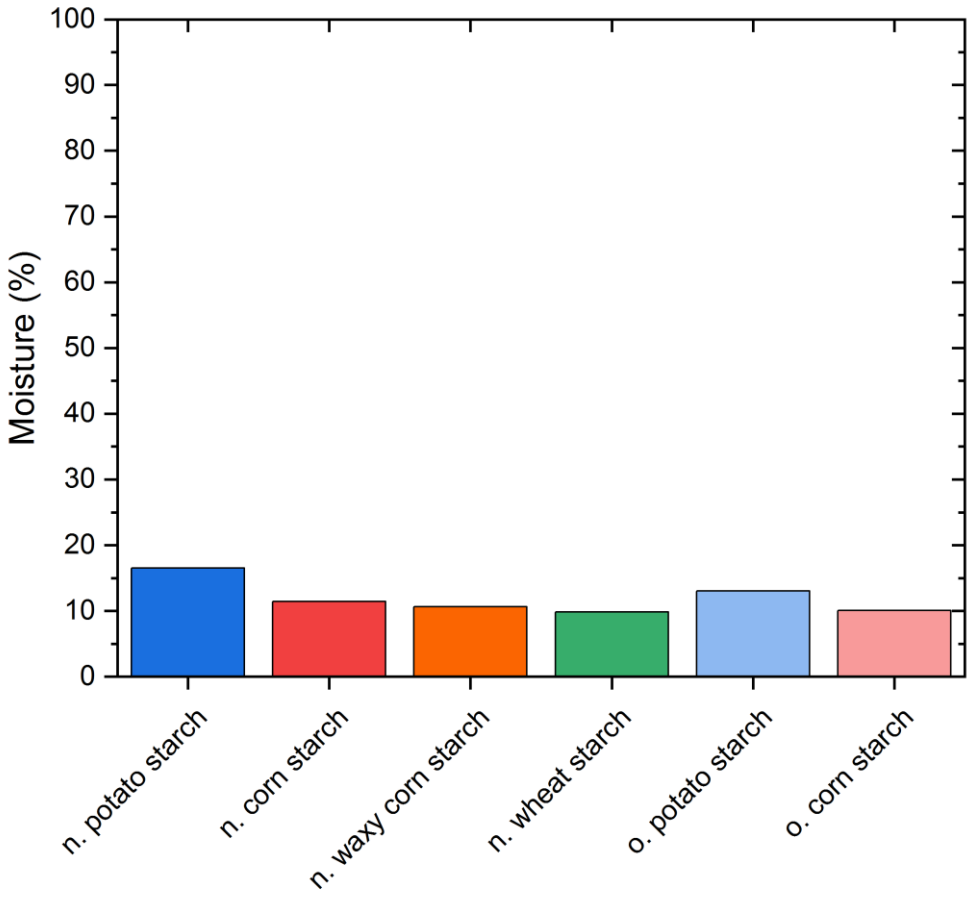

Figure S3. Moisture analysis of the samples carried out at 150 °C.

1.1.3 Particle Size Measurement in Dry State

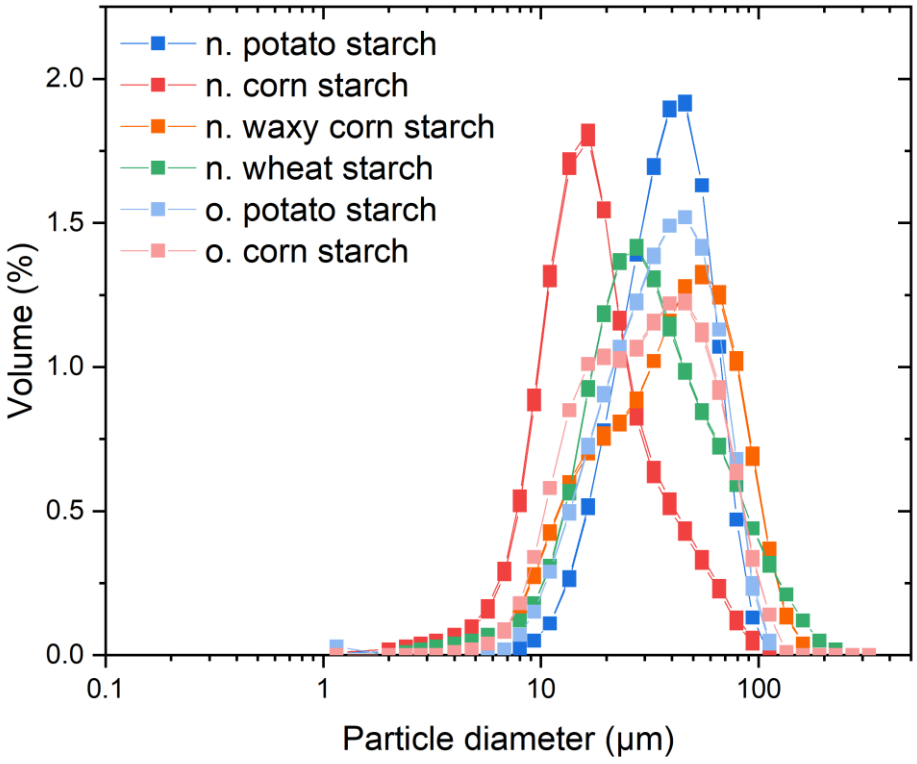

Figure S4. Particle size distribution of the starch samples in dry state.

1.1.4 SEM-EDX analyses of the starch samples before adsorption

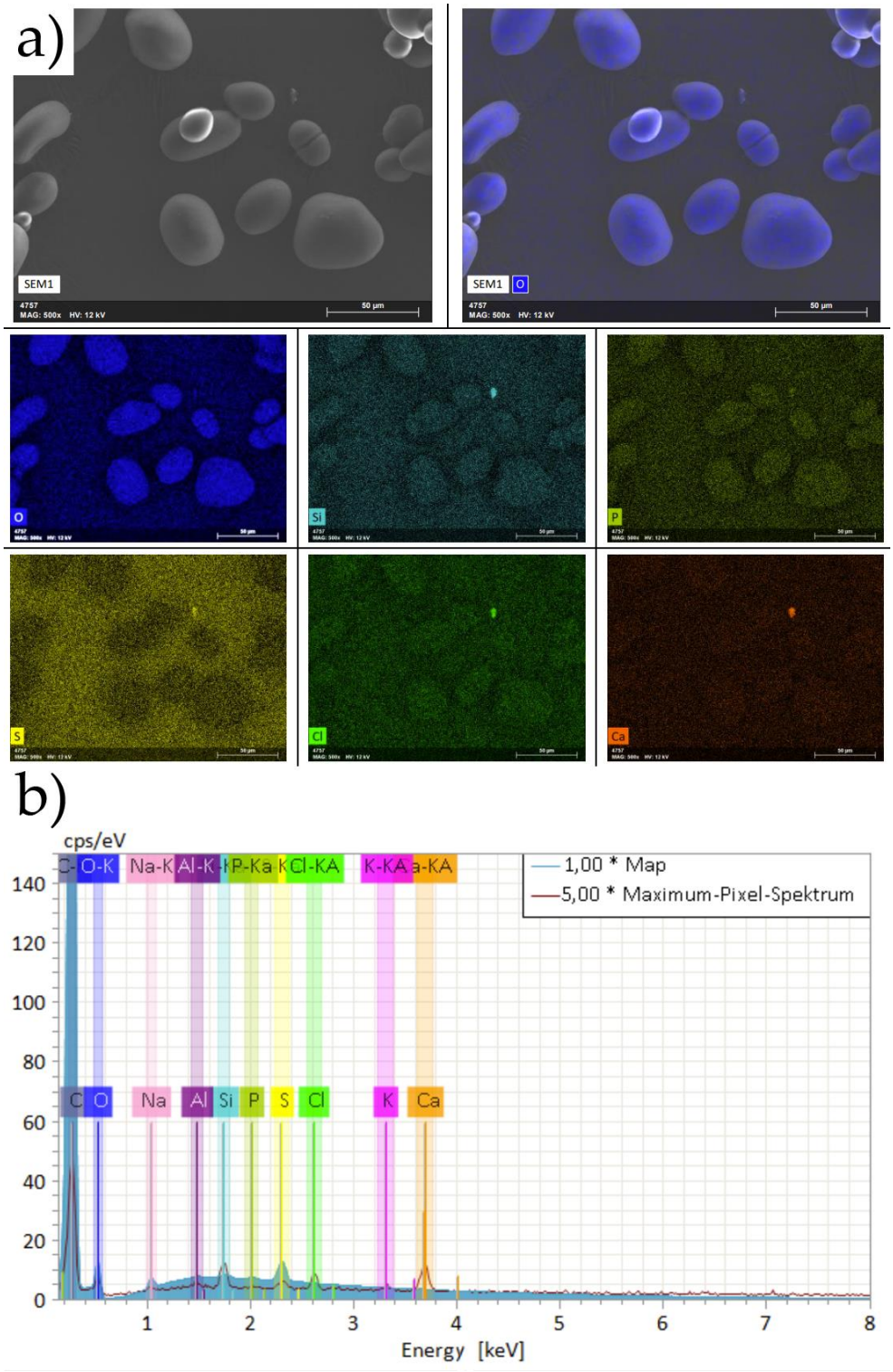

Figure S5. (**a**) SEM images and SEM-EDX elemental mappings from native potato starch, (**b**) sum spectrum (blue) and maximum pixel spectrum (red).

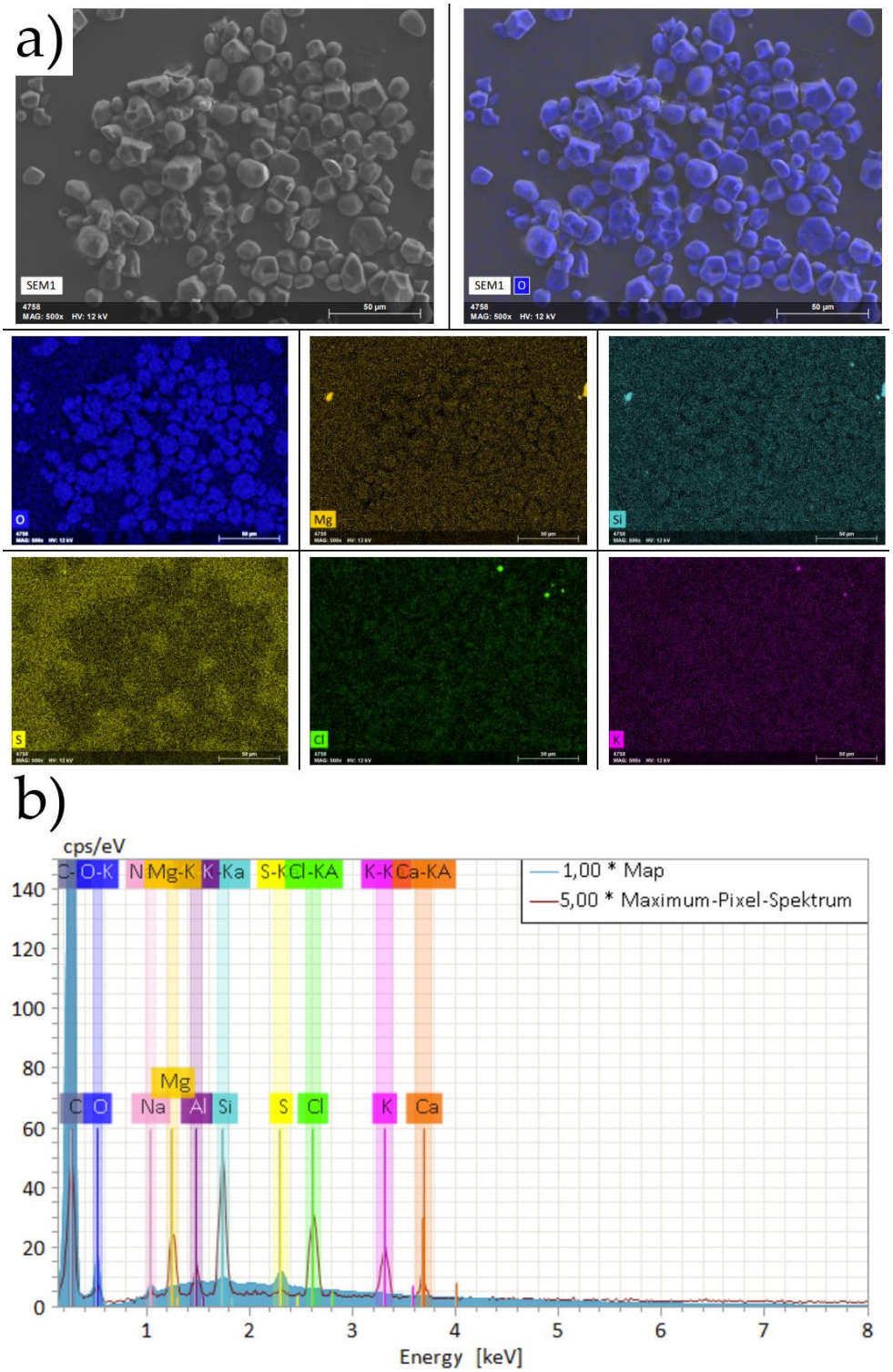

Figure S6. (**a**) SEM images and SEM-EDX elemental mappings from native corn starch, (**b**) sum spectrum (blue) and maximum pixel spectrum (red).

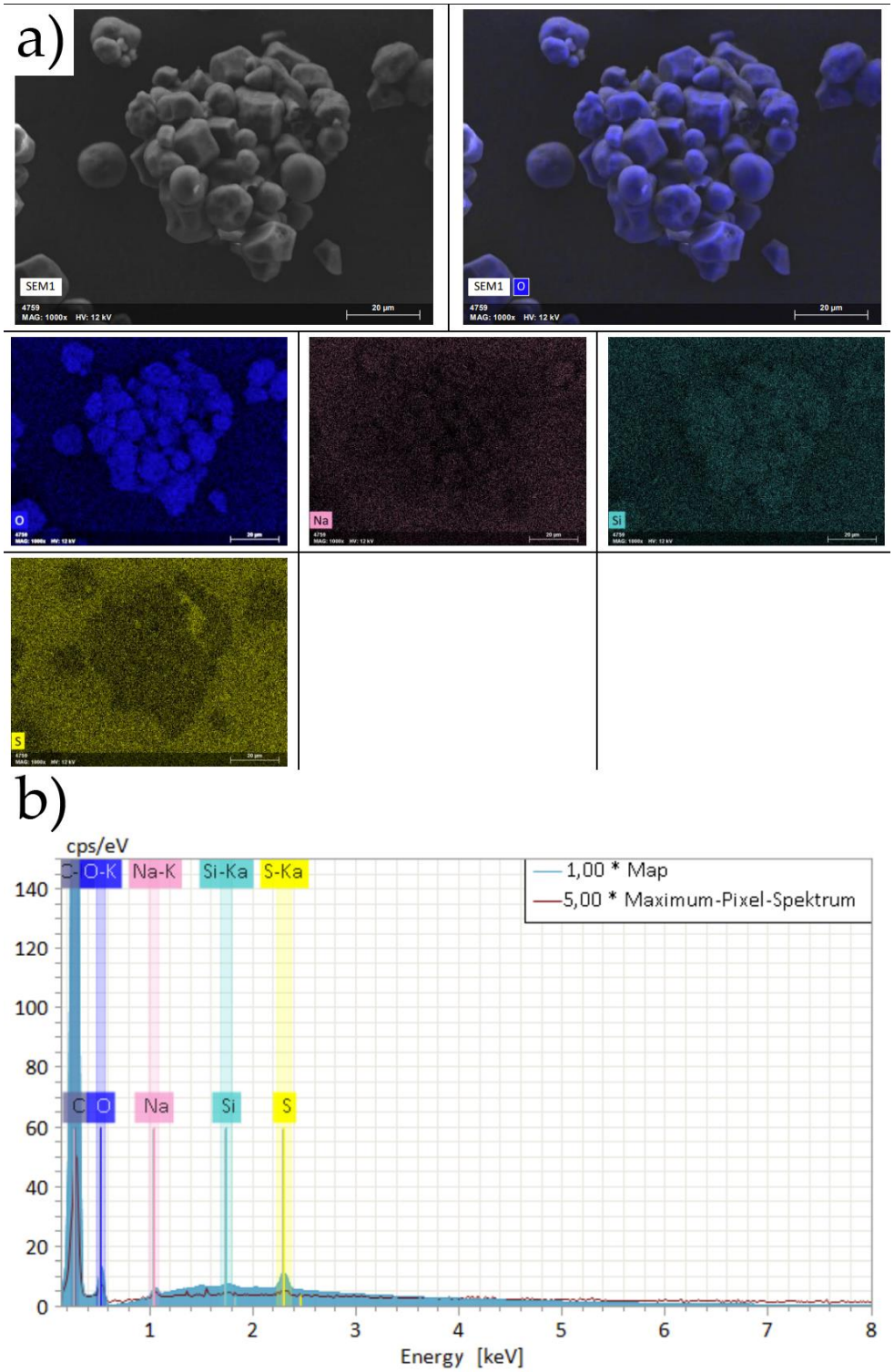

Figure S7. (**a**) SEM images and SEM-EDX elemental mappings from native waxy corn starch, (**b**) sum spectrum (blue) and as maximum pixel spectrum (red).

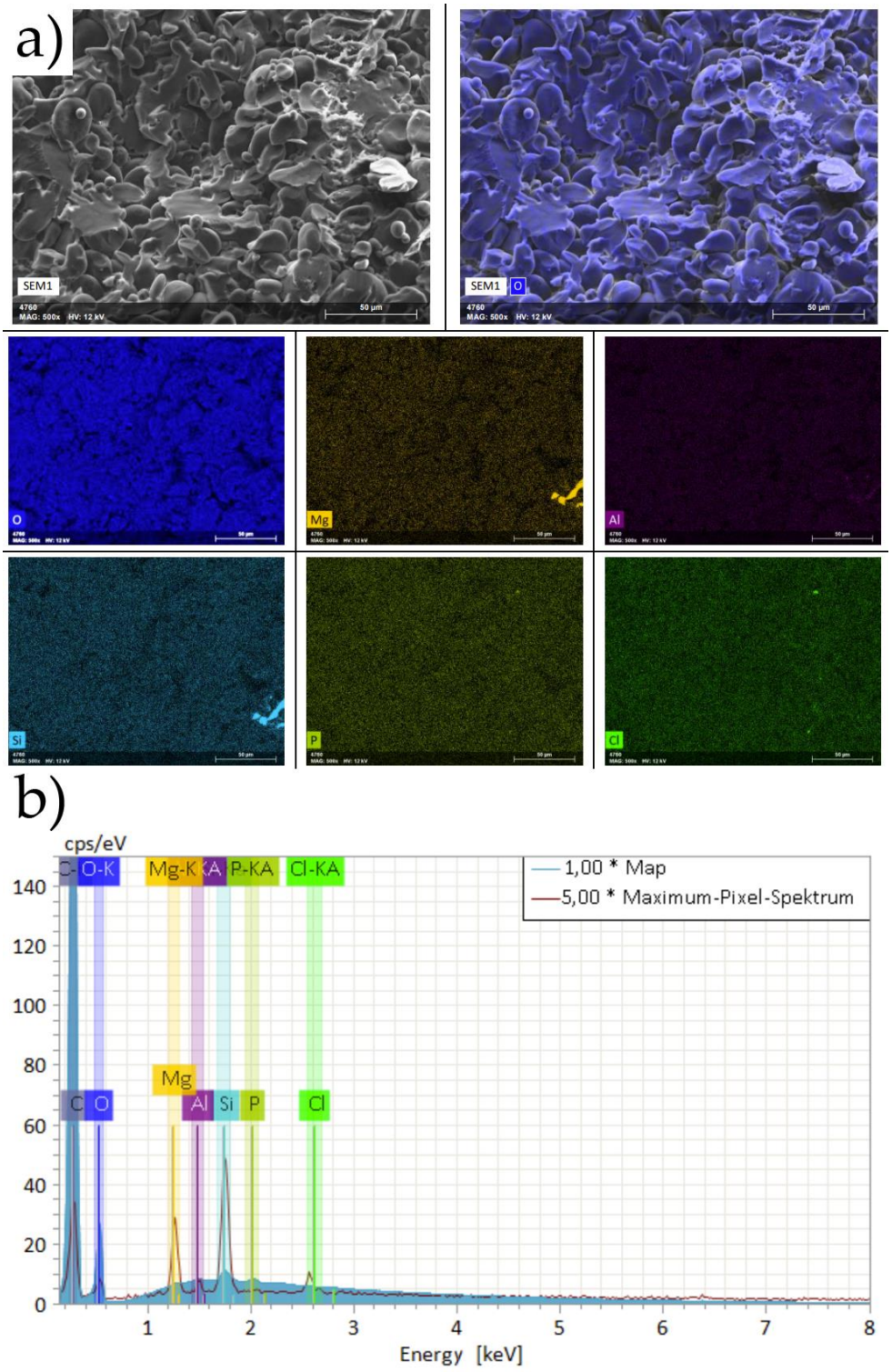

Figure S8. (**a**) SEM images and SEM-EDX elemental mappings from native wheat starch, (**b**) sum spectrum (blue) and maximum pixel spectrum (red).

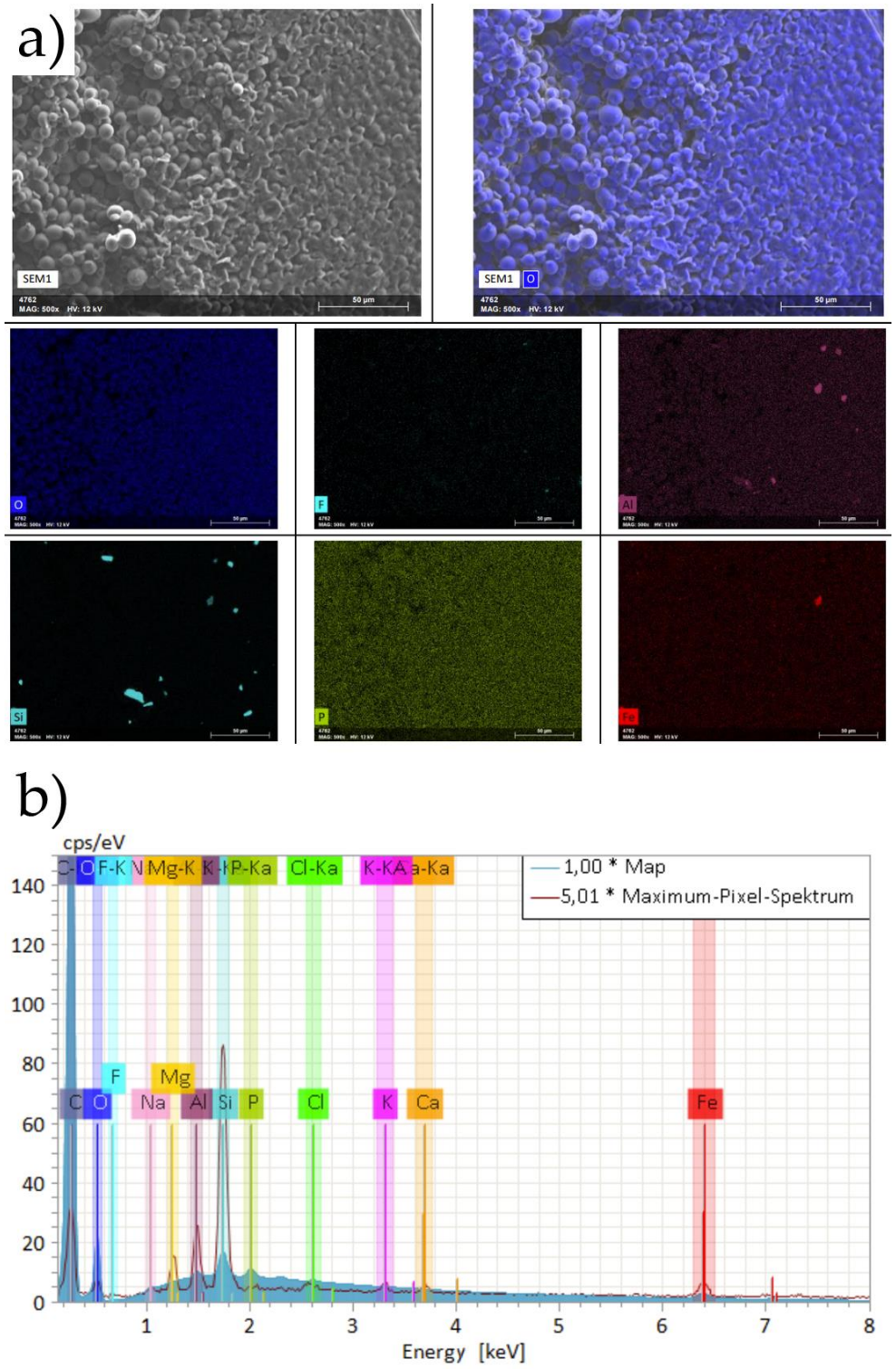

Figure S9. (**a**) SEM images and SEM-EDX elemental mappings from oxidized potato starch, (**b**) sum spectrum (blue) and maximum pixel spectrum (red).

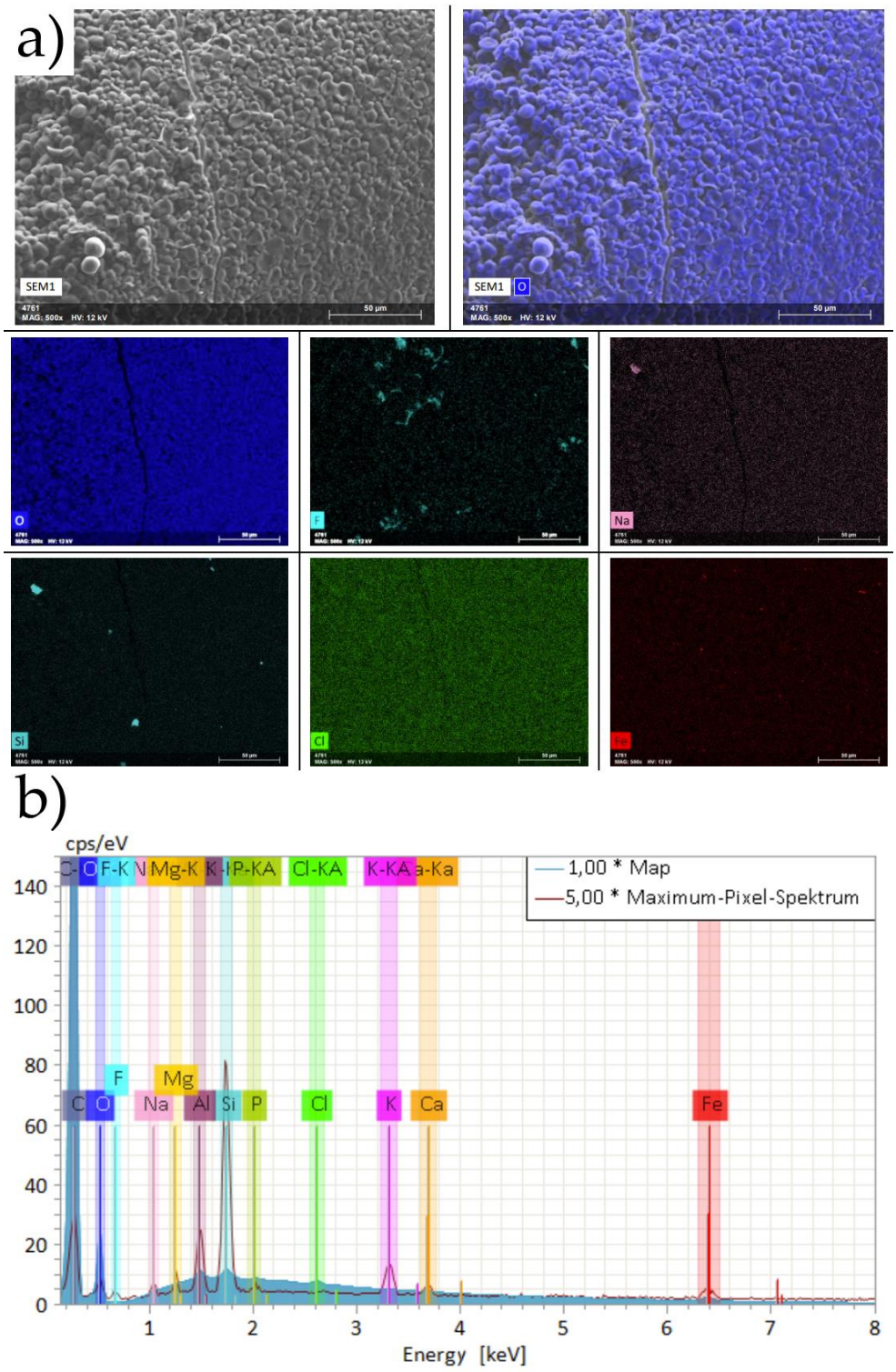

Figure S10. (**a**) SEM images and SEM-EDX elemental mappings from oxidized corn starch, (**b**) sum spectrum (blue) and maximum pixel spectrum (red).

1.1.5 Gas Sorption Analysis and Pore Size Distribution

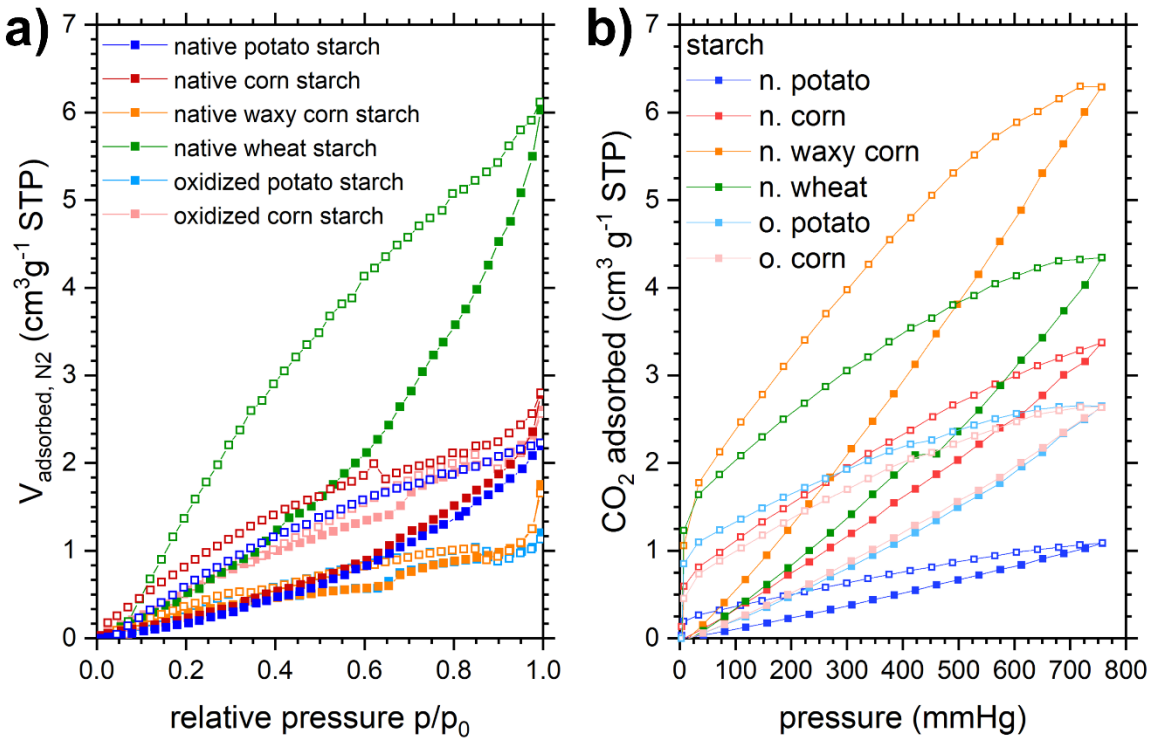

Figure S11. (**a**) Nitrogen sorption isotherms at 77 K and (**b**) carbon dioxide sorption isotherms at 273 K of native potato starch (blue), native corn starch (red), native waxy corn starch (orange), native wheat starch (green), oxidized potato starch (light blue) and oxidized corn starch (pink).

1.2 Adsorption Experiments

1.2.1 pH Values before and after the Sorption Processes of Screening Experiments with Al^{3+}, Pb^{2+} and Cd^{2+}

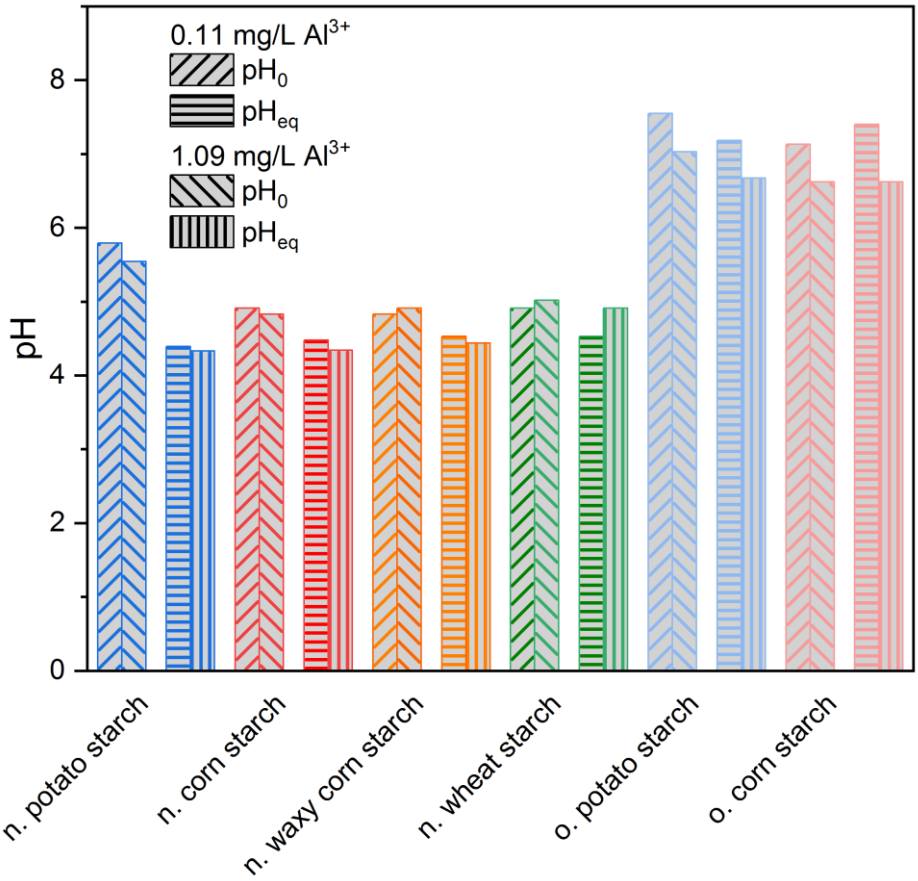

Figure S12. pH values for the experiments with $Al_2(SO_4)_3$ solution of 0.11 mg/L and 1.09 mg/L Al^{3+} before (pH_0) and after (pH_{eq}) the adsorption process of native potato starch (blue), native corn starch (red), native waxy corn starch (orange), native wheat starch (green), oxidized potato starch (light blue) and oxidized corn starch (pink). pH_0 corresponds to the pH value of the adsorptive solution before the experiment and pH_{eq} corresponds to the pH value after the adsorption process.

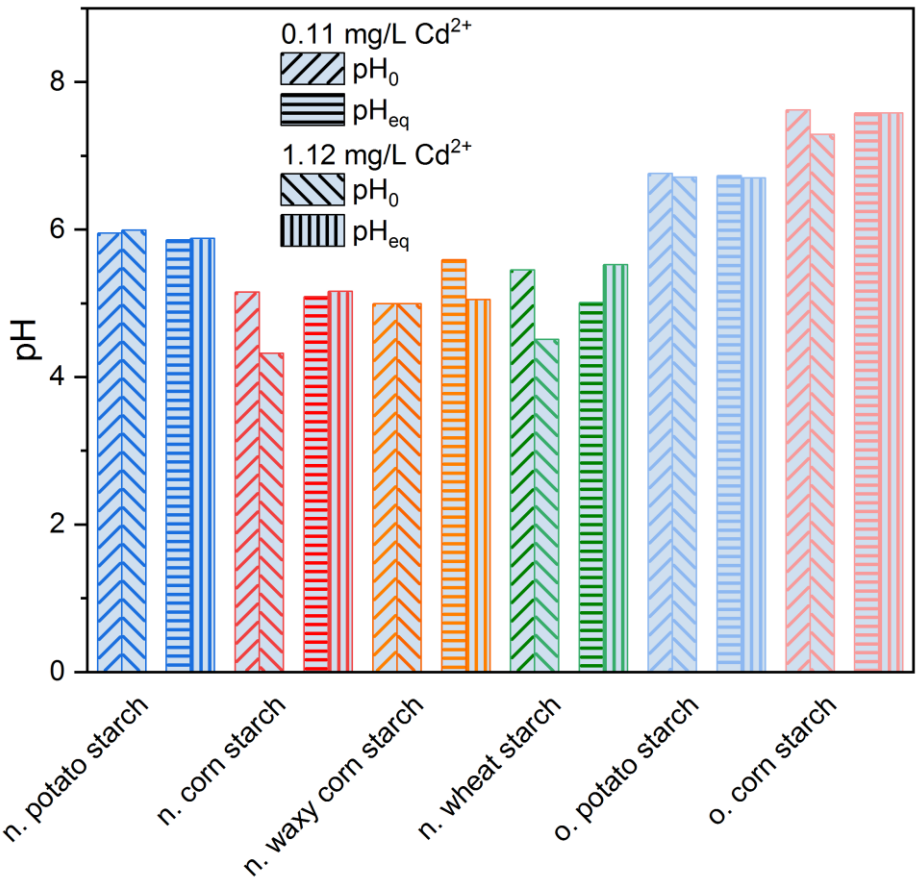

Figure S13. pH values for the experiments with $CdSO_4$ solution of 0.11 mg/L and 1.12 mg/L Cd^{2+} before (pH_0) and after (pH_{eq}) the adsorption process of native potato starch (blue), native corn starch (red), native waxy corn starch (orange), native wheat starch (green), oxidized potato starch (light blue) and oxidized corn starch (pink). pH_0 corresponds to the pH value of the adsorptive solution before the experiment and pH_{eq} corresponds to the pH value after the adsorption process.

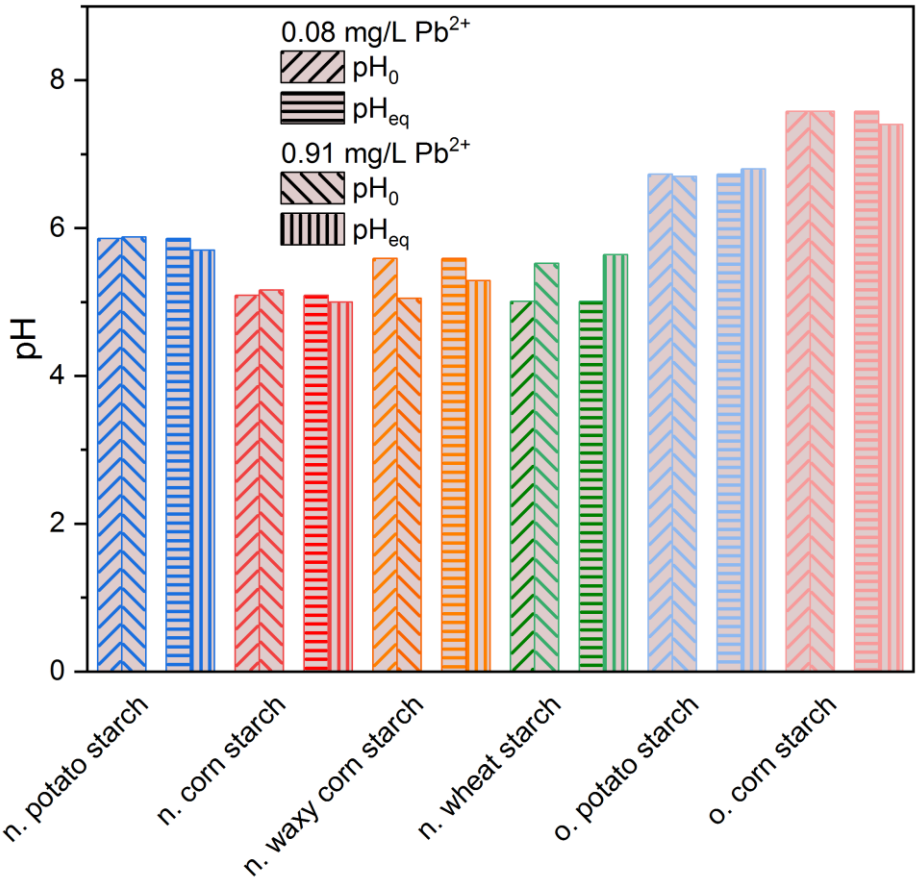

Figure S14. pH values for the experiments with $PbSO_4$ solution of 0.08 mg/L and 0.91 mg/L Pb^{2+} before (pH_0) and after (pH_{eq}) the adsorption process of native potato starch (blue), native corn starch (red), native waxy corn starch (orange), native wheat starch (green), oxidized potato starch (light blue) and oxidized corn starch (pink). pH_0 corresponds to the pH value of the adsorptive solution before the experiment and pH_{eq} corresponds to the pH value after the adsorption process.

1.2.2 Sulfate Adsorption in Screening Experiments with Al^{3+}, Pb^{2+} and Cd^{2+}

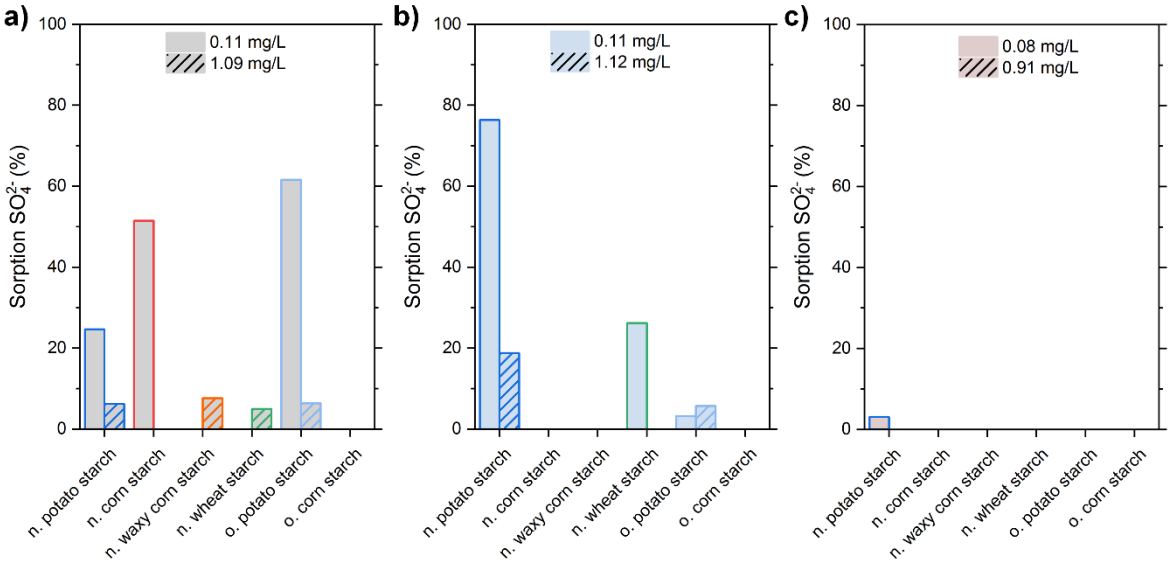

Figure S15. Percentage adsorption of SO_4^{2-} ions from (a) $Al_2(SO_4)_3$ adsorption experiments with an initial concentration of aluminum ions of 0.11 mg/L (solid) and 1.09 mg/L (striped); (**b**) $CdSO_4$ adsorption experiments with an initial concentration of cadmium ions of 0.11 mg/L (solid) and 1.12 mg/L (striped); (**c**) $PbSO_4$ adsorption experiments with an initial concentration of lead ions of 0.08 mg/L (solid) and 0.91 mg/L(striped) onto native potato starch (blue), native corn starch (red), native waxy corn starch (orange), native wheat starch (green), oxidized potato starch (light blue) and oxidized corn starch (pink) in screening experiments with Al^{3+}, Pb^{2+}, and Cd^{2+}.

1.2.3 Sulfate Adsorption and pH Values before and after the Adsorption Process in Sorption Isotherm Experiments with Al^{3+}, Pb^{2+}, and Cd^{2+}

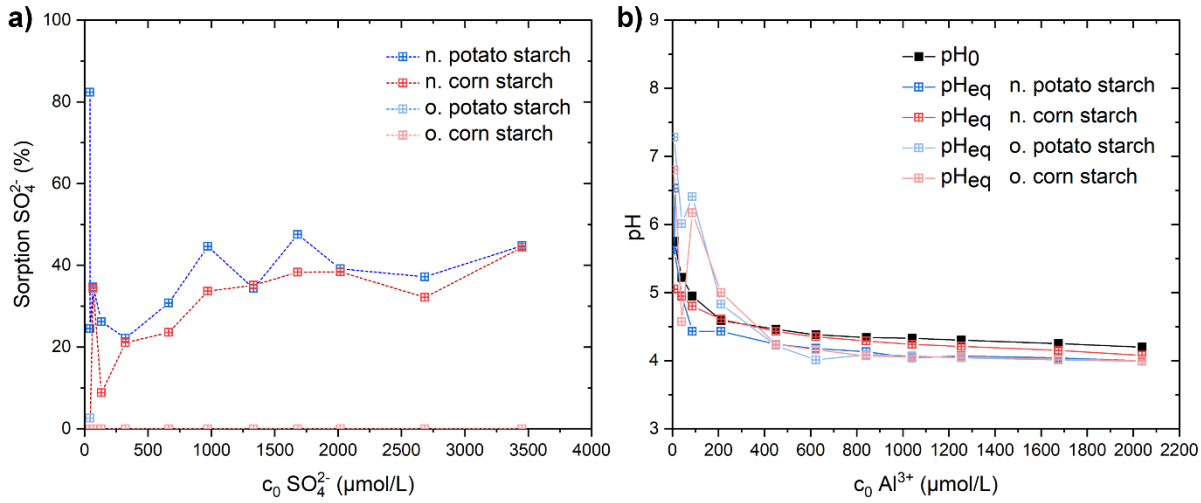

Figure S16. (**a**) SO_4^{2-} percentage adsorption and (**b**) corresponding pH_0 and pH_{eq} values from adsorption of $Al_2(SO_4)_3$ solution onto the starch samples with native potato starch (blue), native corn starch (red), oxidized potato starch (light blue) and oxidized corn starch (pink). pH_0 (black) corresponds to the pH value of the adsorptive solution before the experiment and pH_{eq} corresponds to the pH value after the adsorption process.

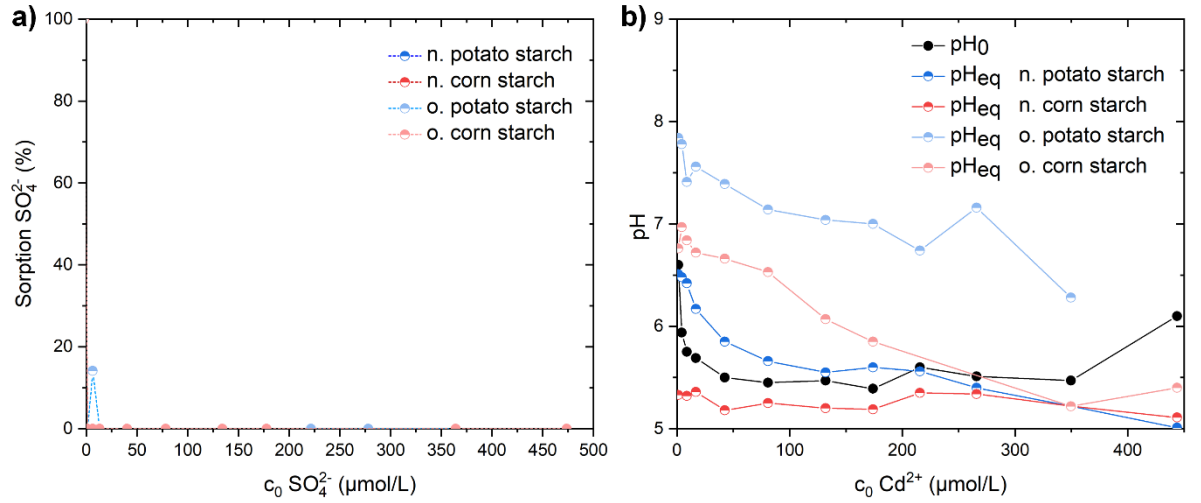

Figure S17. (**a**) SO_4^{2-} percentage adsorption and (**b**) corresponding pH_0 and pH_{eq} values from adsorption of $CdSO_4$ solution onto the starch samples with native potato starch (blue), native corn starch (red), oxidized potato starch (light blue) and oxidized corn starch (pink). pH_0 (black) corresponds to the pH value of the adsorptive solution before the experiment and pH_{eq} corresponds to the pH value after the adsorption process.

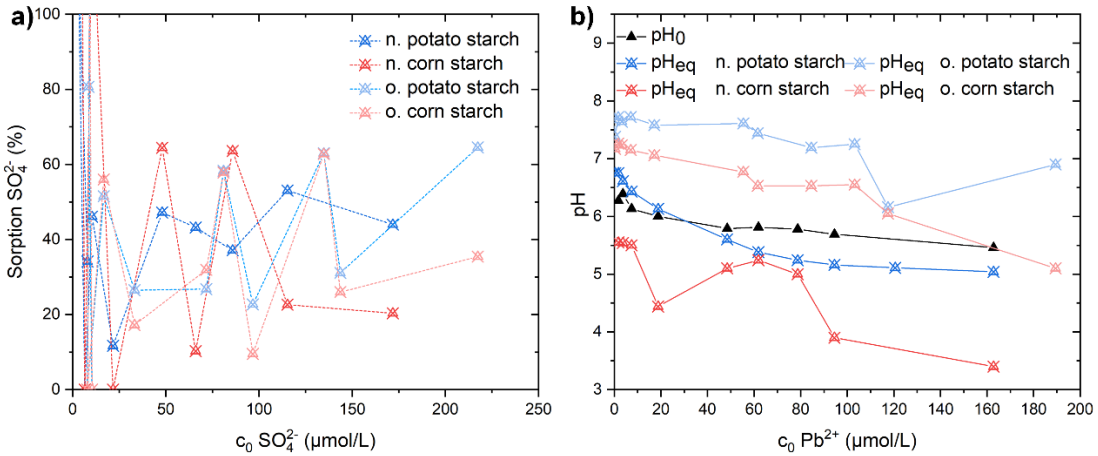

Figure S18. (**a**) SO_4^{2-} percentage adsorption and (**b**) corresponding pH_0 and pH_{eq} values from adsorption of $PbSO_4$ solution onto the starch samples with native potato starch (blue), native corn starch (red), oxidized potato starch (light blue) and oxidized corn starch (pink). pH_0 (black) corresponds to the pH value of the adsorptive solution before the experiment and pH_{eq} corresponds to the pH value after the adsorption process.

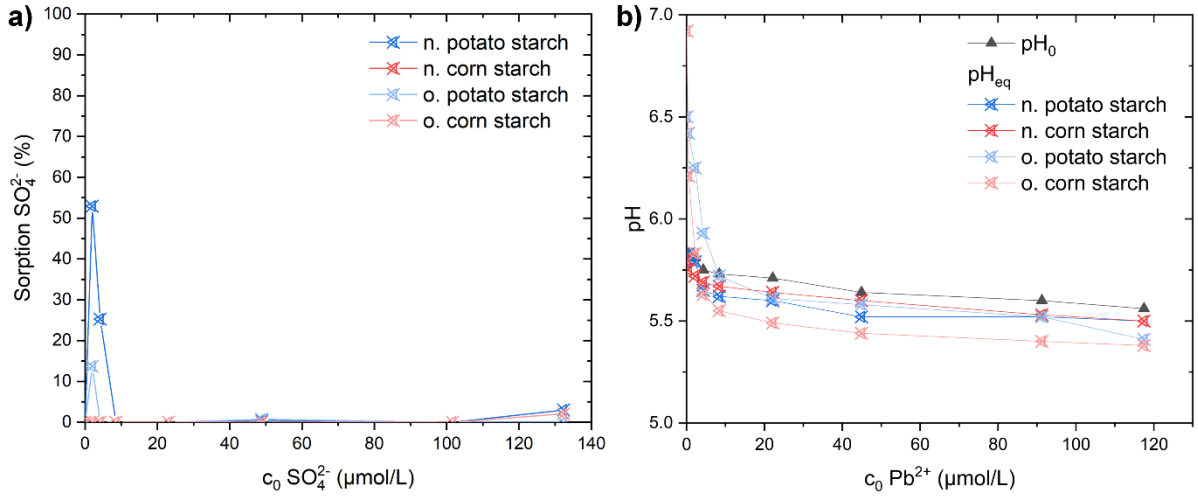

Figure S19. (**a**) SO_4^{2-} percentage adsorption and (**b**) corresponding pH_0 and pH_{eq} values from adsorption of $PbSO_4$ solution onto 10 mg of the starch samples with native potato starch (blue), native corn starch (red), oxidized potato starch (light blue) and oxidized corn starch (pink). pH_0 (black) corresponds to the pH value of the adsorptive solution before the experiment and pH_{eq} corresponds to the pH value after the adsorption process.

1.2.4 SEM-EDX Analysis of Samples after Adsorption

Spot analysis of oxidized potato starch (10 mg/ 30 mL adsorbent dose) after adsorption experiment with $PbSO_4$ solution:

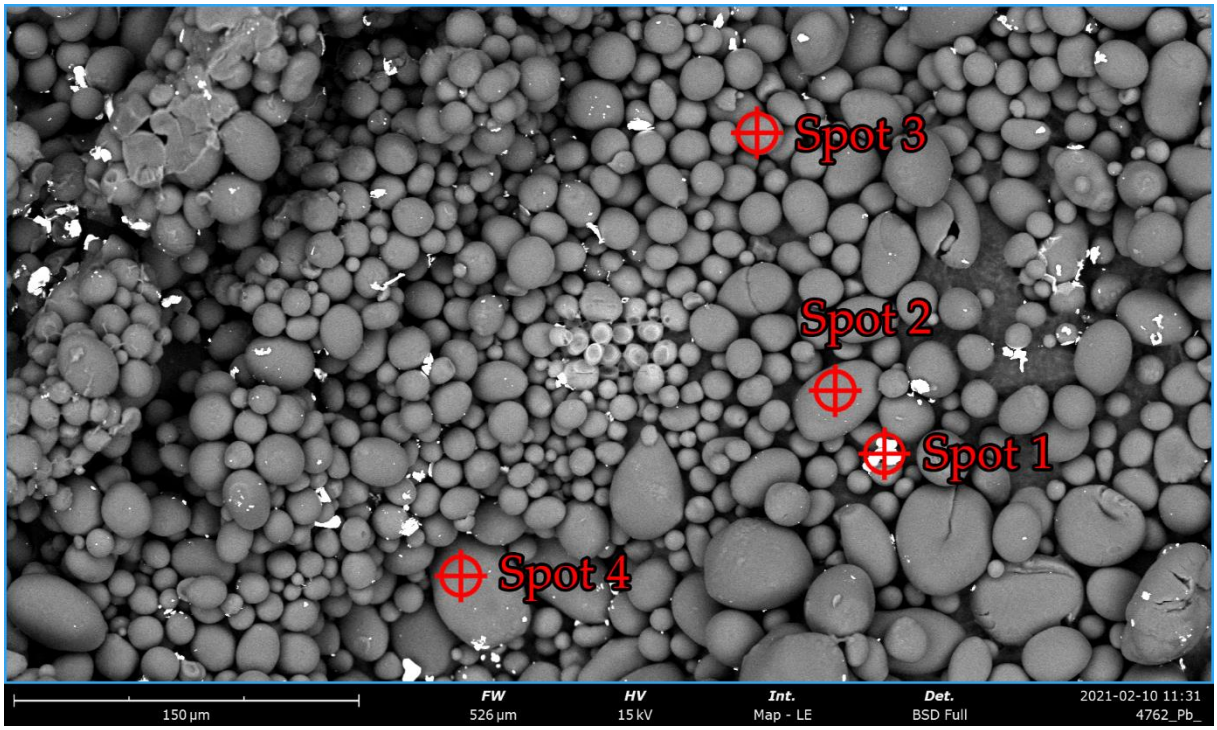

Figure S20. SEM image of oxidized potato starch (10 mg/ 30 mL adsorbent dose) after adsorption experiment with $PbSO_4$ solution at 1000 fold magnification with the location of the following spot analysis by EDS.

Table S2. Relative atomic concentration derived from spot analyses (location in Figure S20) at oxidized potato starch (10 mg/ 30 mL adsorbent dose) after adsorption experiment with $PbSO_4$ solution.

Element Symbol	Element Name	Atomic Concentration in Rel. Atomic%				
		Map	Spot 1	Spot 2	Spot 3	Spot 4
C	Carbon	54.2	61.9	75.6	77.6	55.5
O	Oxygen	45.6	29.9	23.7	22.0	44.0
Pb	Lead	0.2	3.1	0.7	0.4	0.5
S	Sulfur	0.0	5.1	0.0	0.0	0.0

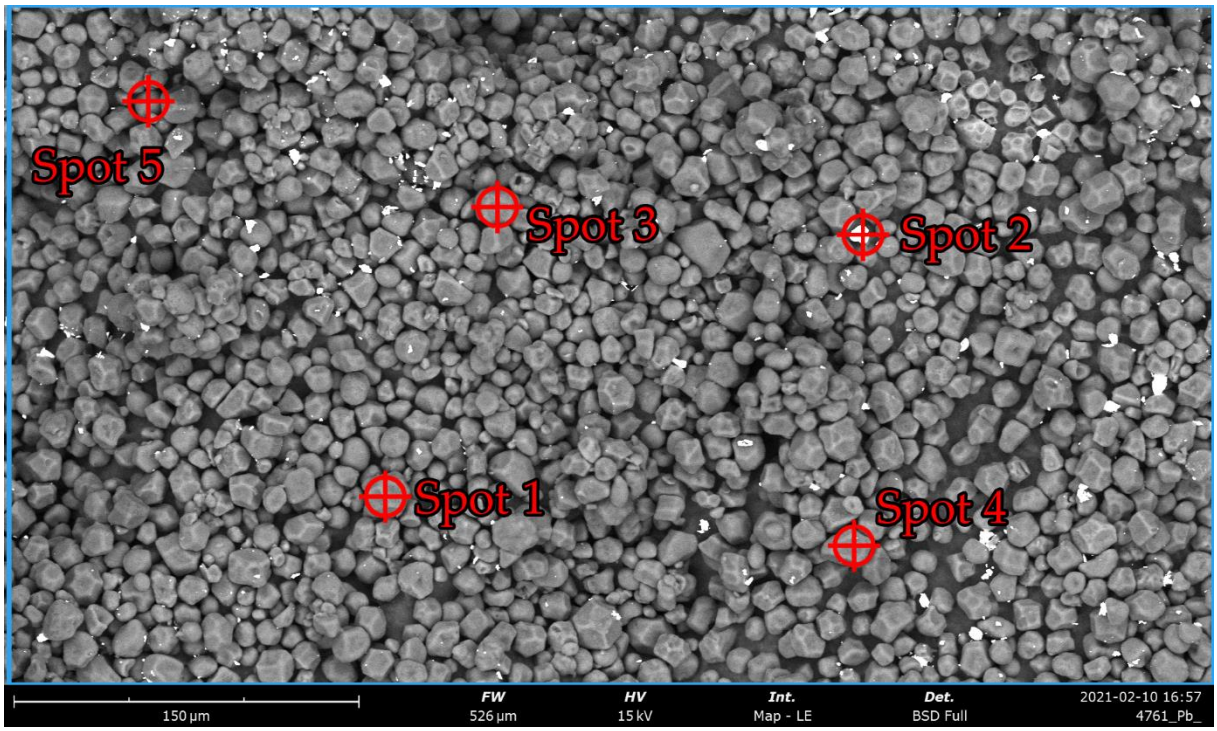

Figure S21. SEM image of oxidized corn starch (10 mg/ 30 mL adsorbent dose) after adsorption experiment with $PbSO_4$ solution at 1000 fold magnification with the location of the following spot analysis by EDS.

Table S3. Relative atomic concentration derived from spot analyses (location in Figure S21) at oxidized corn starch (10 mg/ 30 mL adsorbent dose) after adsorption experiment with $PbSO_4$ solution.

Element Symbol	Element Name	Atomic Concentration in Rel. Atomic%					
		Map	Spot 1	Spot 2	Spot 3	Spot 4	Spot 5
C	Carbon	52.4	73.4	58.6	64.4	68.2	75.4
O	Oxygen	47.4	26.2	27.5	34.9	31.1	24.3
Pb	Lead	0.2	0.4	5.2	0.7	0.7	0.3
S	Sulfur	0.0	0.0	8.6	0.0	0.0	0.0

1.3 Comparison of Fitting Models for Sorption Isotherm Experiments with Al^{3+}, Pb^{2+}, and Cd^{2+}

1.3.2 Fittings for Al^{3+} Sorption Isotherms

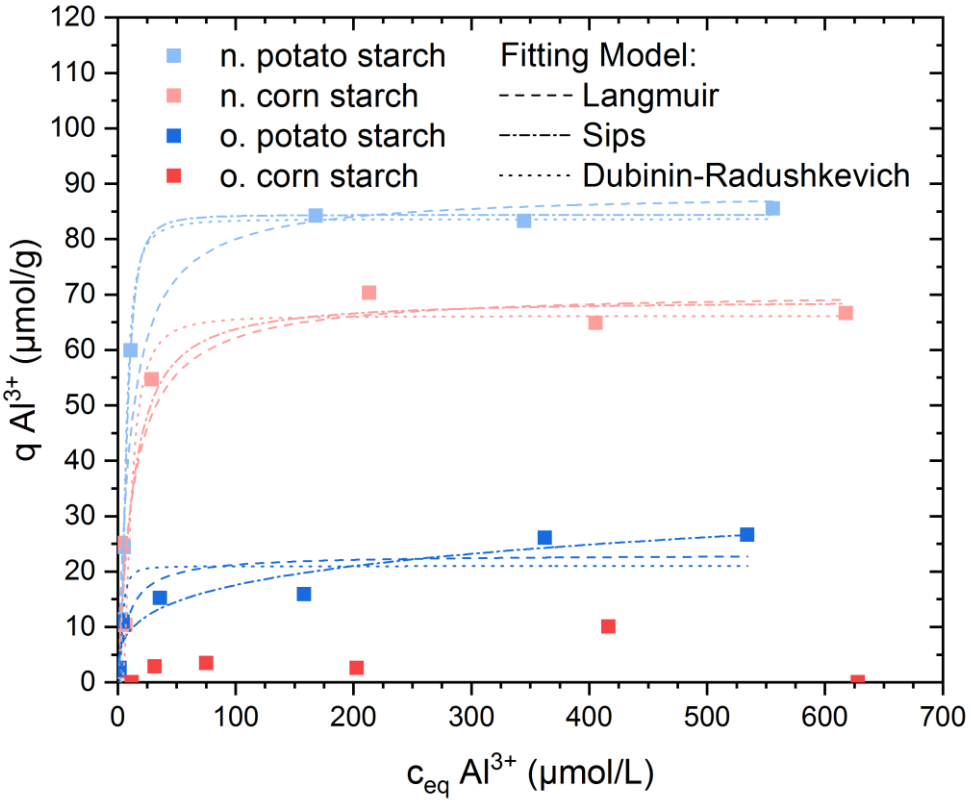

Figure S22. Comparison of isotherms fitted for the Langmuir, Sips and Dubinin-Radushkevich models for the adsorption of Al^{3+} from $Al_2(SO_4)_3$ solution with native potato starch (blue), oxidized potato starch (light blue) and oxidized corn starch (pink). Native corn starch (red) does not exhibit a viable fitting for the above mentioned models.

1.3.3 Fittings for Cd^{2+} Sorption Isotherms

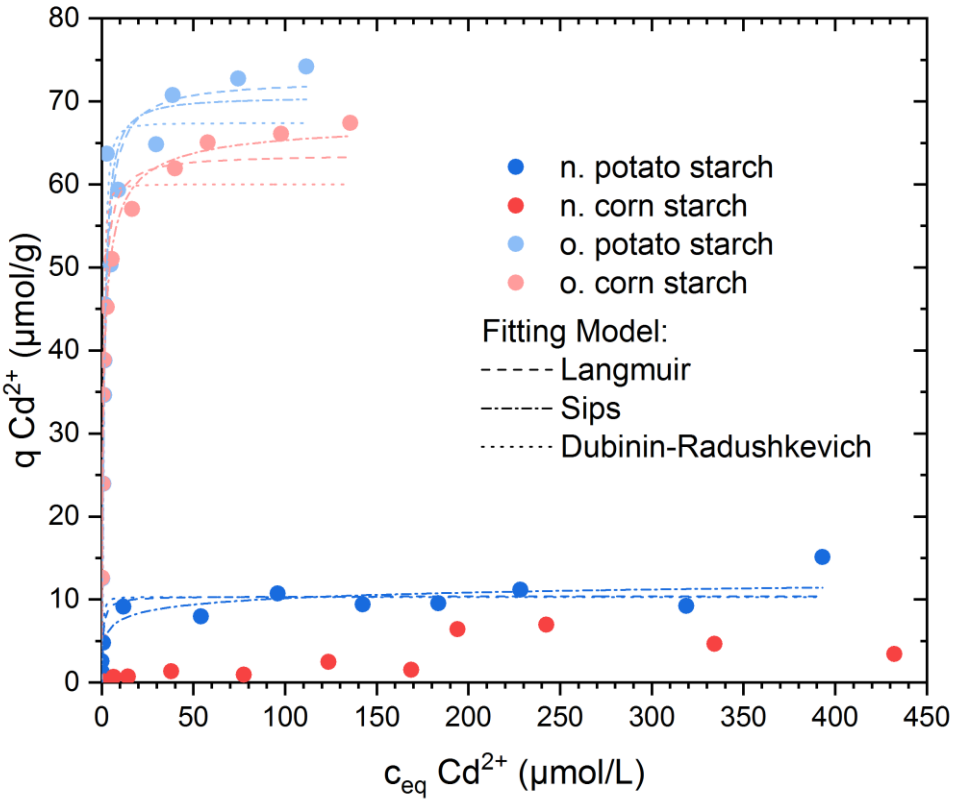

Figure S23. Comparison of isotherms fitted for the Langmuir, Sips and Dubinin-Radushkevich model for the adsorption of Cd^{2+} from $CdSO_4$ solution with native potato starch (blue), oxidized potato starch (light blue) and oxidized corn starch (pink). Native corn starch (red) does not exhibit a viable fitting for the above mentioned models ($R^2 < 0.7$).

1.3.4 Fittings for Pb^{2+} Sorption Isotherms

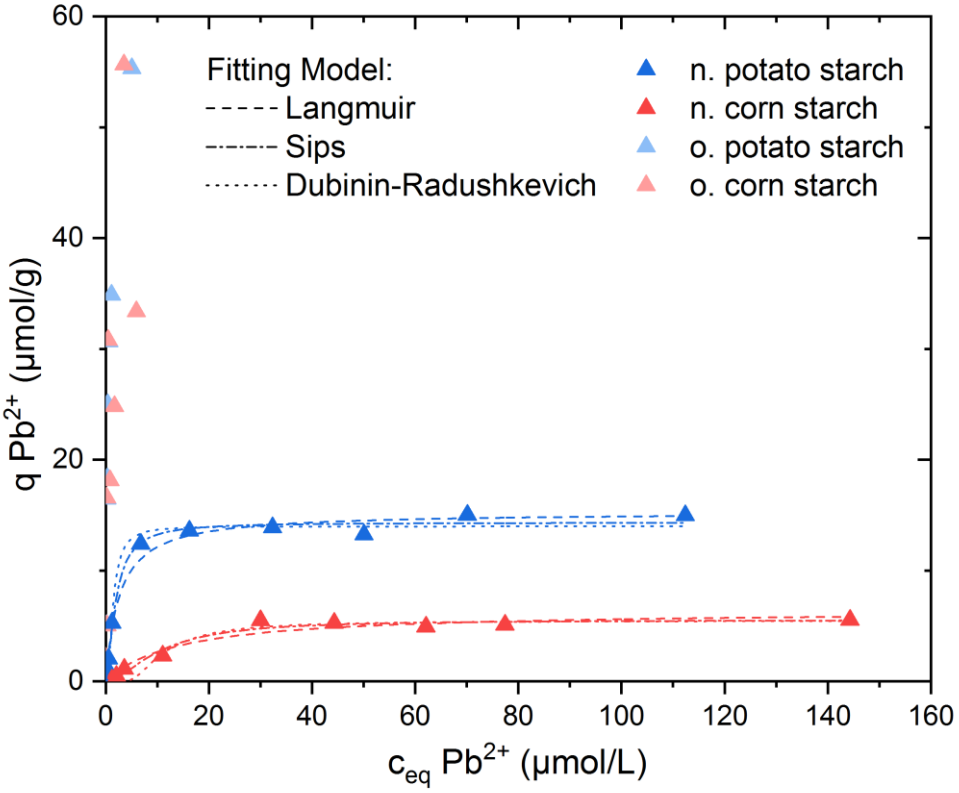

Figure S24. Comparison of isotherms fitted for the Langmuir, Sips and Dubinin-Radushkevich model for the adsorption of Pb^{2+} from $PbSO_4$ solution with adsorbent doses of 100 mg/ 30mL of the respective starch. Native potato starch is shown in blue and native corn starch in red. Oxidized corn starch (pink) and oxidized potato starch (light blue) were not fitted due to not reaching a plateau.

1.3.4 Fittings for Pb^{2+} Sorption Isotherms

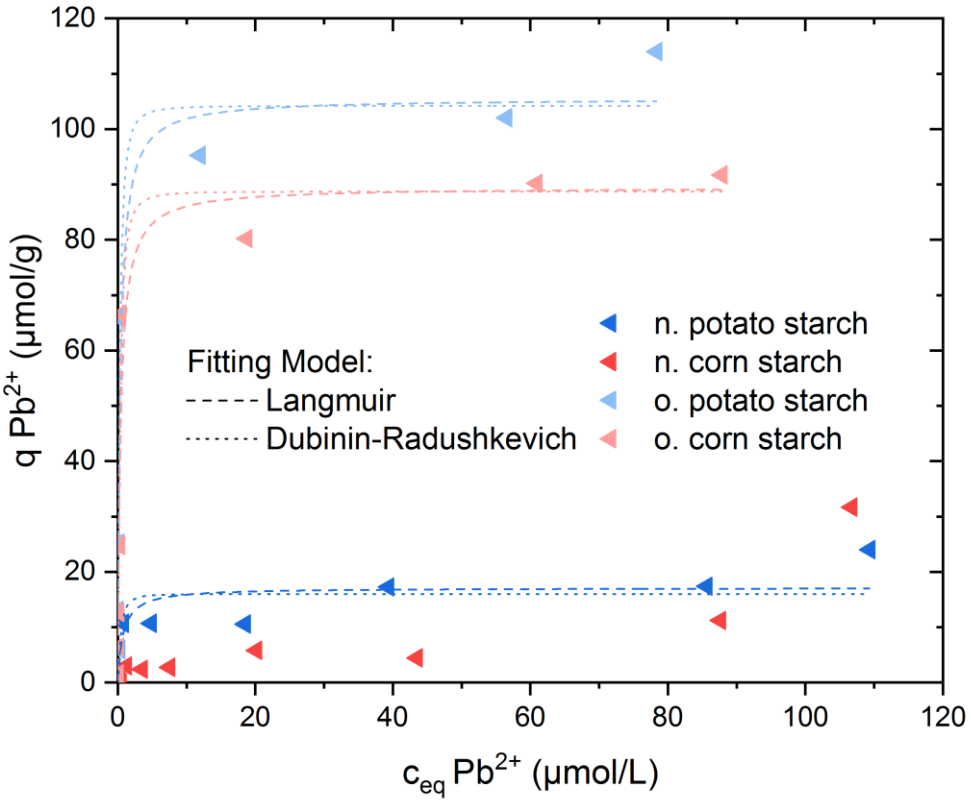

Figure S25. Comparison of isotherms fitted for the Langmuir and Dubinin-Radushkevich model for the adsorption of Pb^{2+} from $PbSO_4$ solution with decreased amounts (10 mg each) of native potato starch (blue), oxidized potato starch (light blue) and oxidized corn starch (pink). Native corn starch (red) does not exhibit a viable fitting for the above mentioned models.

1.4 Sorption Experiments with Real Water Samples

1.4.1 Characterization of Real wWater Samples

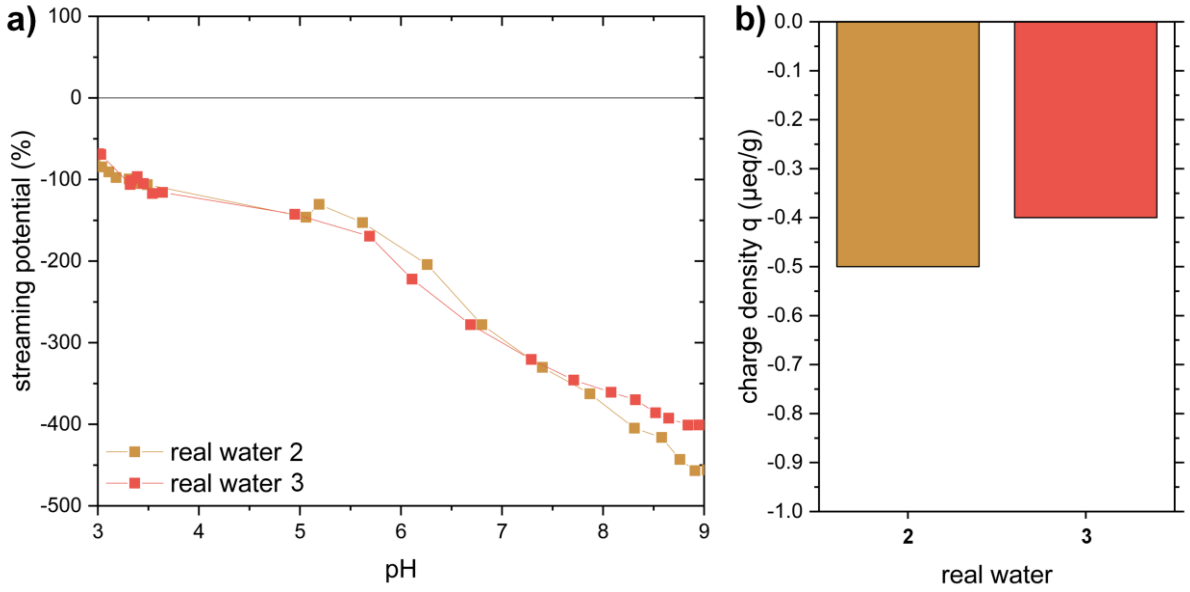

Figure S26. (**a**) Streaming potential vs. pH curves and (**b**) charge densities at pH value of 3.6 of water 2 (brown) and water 3 (red).

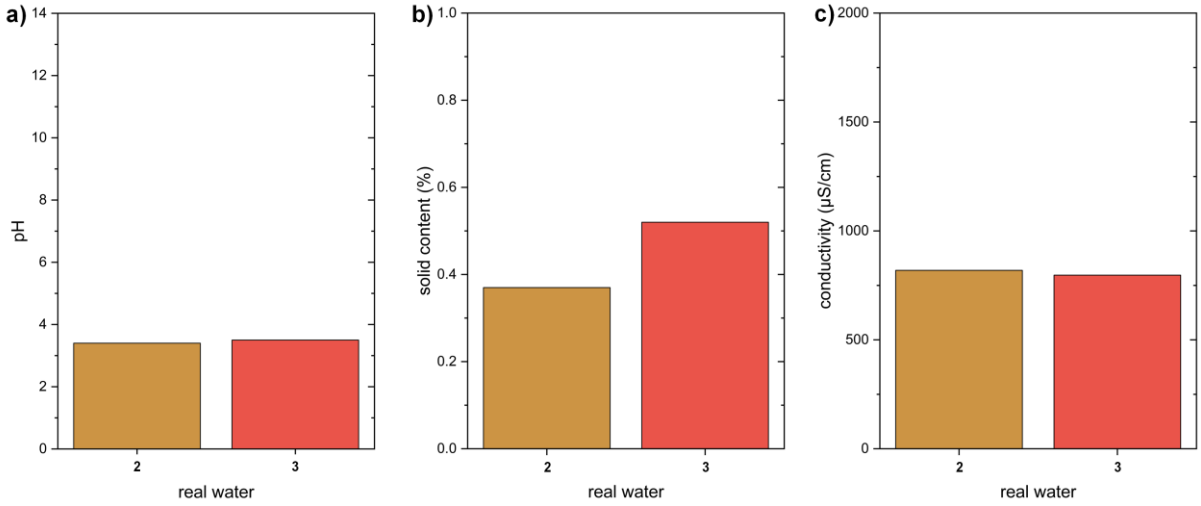

Figure S27. (**a**) pH values for the water samples with water 2 is shown in brown and water 3 is shown in red, (**b**) Solid content in % in water 2 and water 3 and (**c**) electrical conductivity of water 2 and 3.

1.4.2 Removal of Al^{3+} with Starch from Real Water Samples

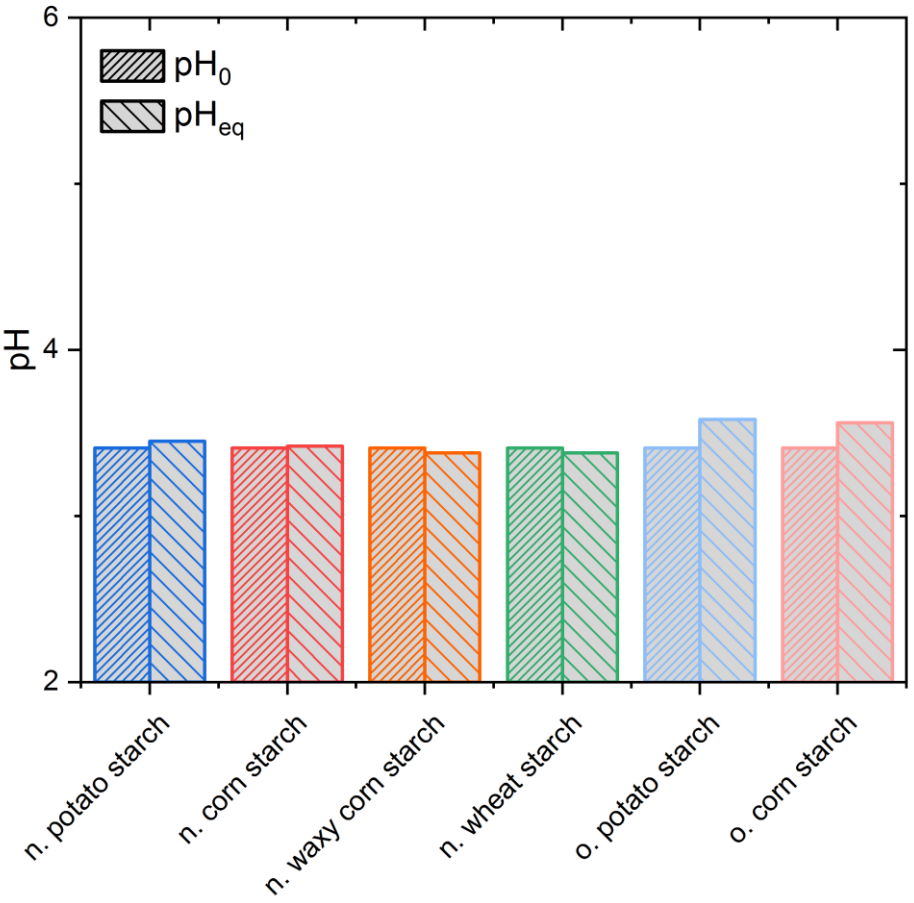

Figure S28. pH_0 and pH_{eq} values from adsorption of Al^{3+} onto the starch samples in real water 1 with native potato starch (blue), native corn starch (red), oxidized potato starch (light blue) and oxidized corn starch (pink). pH_0 corresponds to the pH value of the adsorptive solution before the experiment and pH_{eq} corresponds to the pH value after the adsorption process.

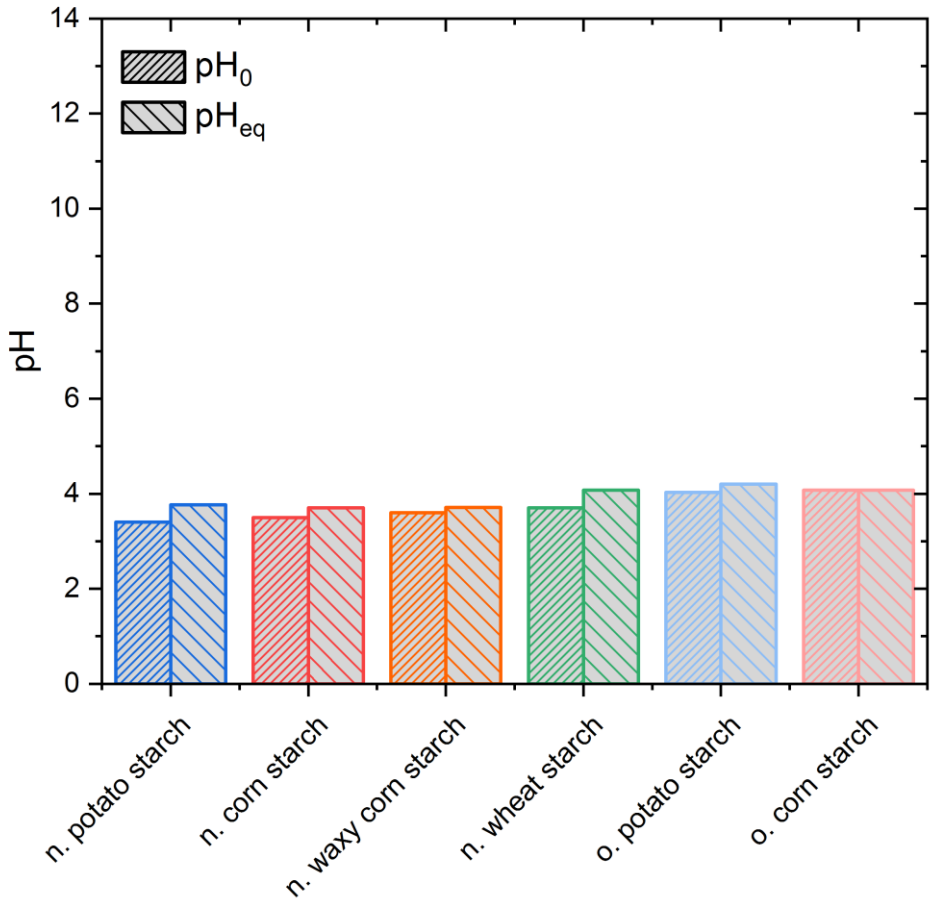

Figure S29. pH_0 and pH_{eq} values from adsorption of Al^{3+} onto the starch samples in real water 2 with native potato starch (blue), native corn starch (red), oxidized potato starch (light blue) and oxidized corn starch (pink). pH_0 corresponds to the pH value of the adsorptive solution before the experiment and pH_{eq} corresponds to the pH value after the adsorption process.

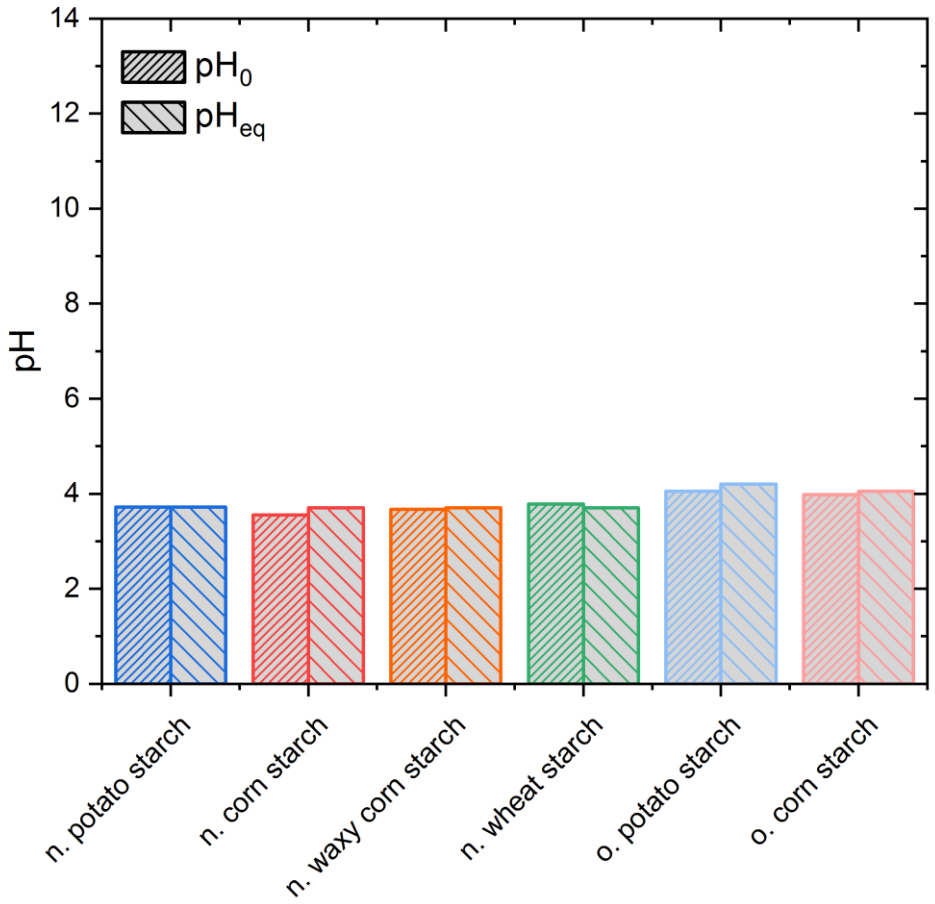

Figure S30. pH_0 and pH_{eq} values from adsorption of Al^{3+} onto the starch samples in real water 3 with native potato starch (blue), native corn starch (red), oxidized potato starch (light blue) and oxidized corn starch (pink). pH_0 corresponds to the pH value of the adsorptive solution before the experiment and pH_{eq} corresponds to the pH value after the adsorption process.

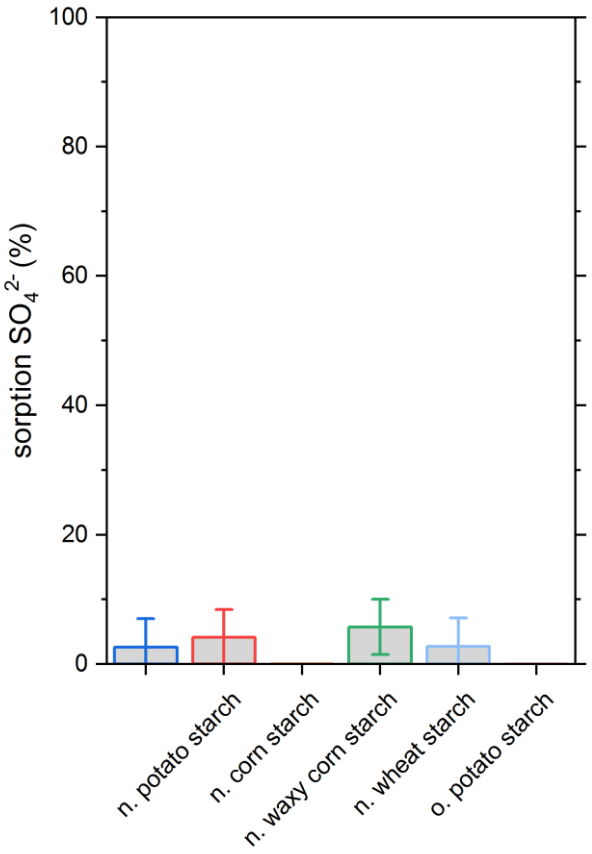

Figure S31. SO_4^{2-} percentage adsorption onto the starch samples in real water 1 with native potato starch (blue), native corn starch (red), oxidized potato starch (light blue) and oxidized corn starch (pink). Also, for reference one blind sample without added adsorber material is presented (black and dashed horizontal line).

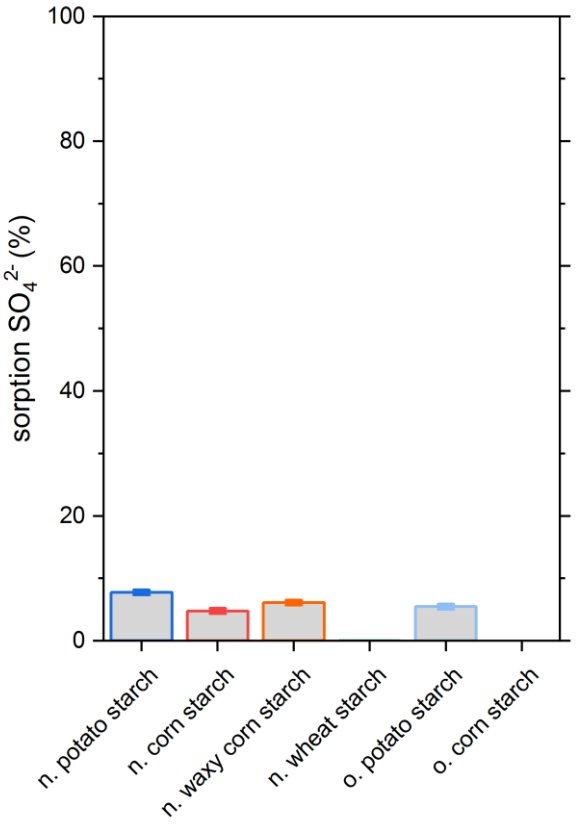

Figure S32. SO_4^{2-} percentage adsorption onto the starch samples in real water 2 with native potato starch (blue), native corn starch (red), oxidized potato starch (light blue) and oxidized corn starch (pink). Also, for reference one blind sample without added adsorber material is presented (black and dashed horizontal line).

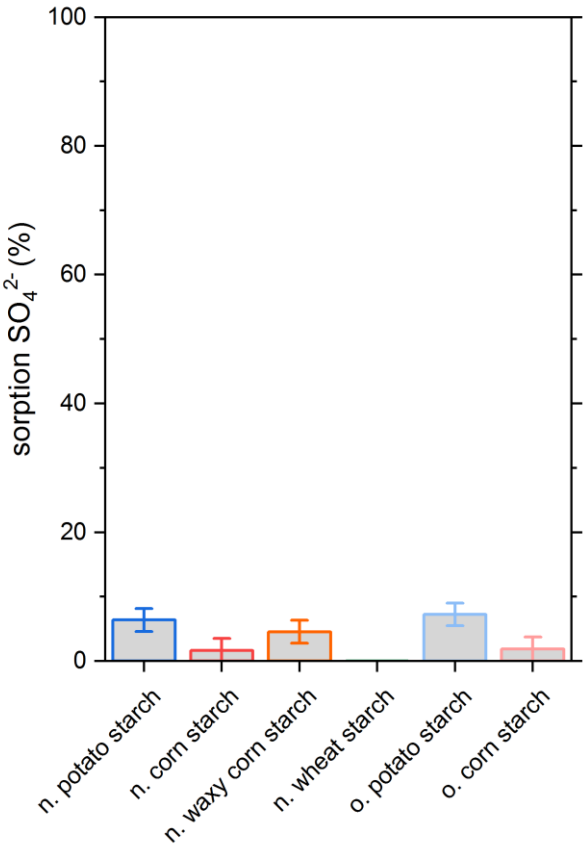

Figure S33. SO_4^{2-} percentage adsorption onto the starch samples in real water3 with native potato starch (blue), native corn starch (red), oxidized potato starch (light blue) and oxidized corn starch (pink). Also, for reference one blind sample without added adsorber material is presented (black and dashed horizontal line).

2. Classification of the Obtained Sorption Capacities with Other Materials

Table S4. Sorption capacities for removal of Al^{3+} compounds from aqueous solutions with different sorbent materials and adsorbent doses (a.d.). The obtained sorption capacities from this work were achieved in the batch adsorption experiments.

Material	Sorption Capacity q (mg/g)	Salt	Experimental Conditions			Ref.
			pH_0	a.d. (g/L)	t, T	
Oxidized potato starch	2.3	$Al_2(SO_4)_3$	4.2	2	2 h, 25 °C	This work
Oxidized corn starch	1.9	$Al_2(SO_4)_3$	4.2	2	2 h, 25 °C	This work
Typha domingensis leaf powder	0.35	n.a.	2.5	10	120 min, 25 °C	[4]
Date-pit activated carbon	5.83	Al-Powder in HCl	4	2	24 h, 22 °C	[5]
BDH activated carbon	6.56	Al-Powder in HCl	4	2	24 h, 22 °C	[5]
L. japonica algae	2.79	Al-$(NO_3)_3$	4.5	1	30 h, -	[6]
PM (PalPower M10)	27.78	Al from waste water	4	35	2h, 25 °C	[7]
Starch	292	$AlCl_3$	7.5	10	90 min, 25 °C	[8]
Chitin (QTN)	15	$(Al_2(SO_4)_3 \cdot (14–18) \cdot H_2O)$	n.a	0.15	2h, 25 °C	[9]
Chitosan (QUIT)	10	$(Al_2(SO_4)_3 \cdot (14–18) \cdot H_2O)$	n.a	0.1	2h, 25 °C	[9]

Table S5. Sorption capacities for removal of Cd^{2+} compounds from aqueous solutions with different sorbent materials and adsorbent doses (a.d.). The obtained sorption capacities from this work were achieved in the batch adsorption experiments.

Material	Sorption Capacity q (mg/g)	Salt	Experimental Conditions			Ref.
			pH_0	a.d. (g/L)	t, T	
Oxidized potato starch	7.9	$CdSO_4 \cdot H_2O$	6.1	2	2 h, 25 °C	This work
Oxidized corn starch	7.7	$CdSO_4 \cdot H_2O$	6.1	2	2 h, 25 °C	This work
Native potato starch	1.6	$CdSO_4 \cdot H_2O$	6.1	2	2 h, 25 °C	This work
Aminopyridine modified poly(styrene-alt-maleic anhydride) (CSMA-AP)	81.30	$CdCl_2 \cdot H_2O$	5	2.5	60 min, 25 °C	[10]
Ficus religiosa Leaf Powder	27.14	$CdSO_4 \cdot 8H_2O$	5	-	30 min, 30 °C	[11]
Aspergillus niger	2.2	$CdSO_4 \cdot 8/3H_2O$	6.01	5.22	24 h, 30 °C	[12]
Polyamide Resin	413.5	$CdSO_4 \cdot 8H_2O$	6	1	60 min, 30 °C	[13]
Carbon prepared from apricot stone (ASAC)	33.57	$CdSO_4 \cdot 8H_2O$	6	2	48 h, 25 °C	[14]
Sporopollenin	1.64	$CdCl_2 \cdot H_2O$	7	16.67	60 min, 20 °C	[15]
L. japonica algae	1.21	$Cd(NO_3)_2$	4.5	1	30 h, -	[6]
Fe_2O_3 NPs-Starch	322.58	$Cd(NO_3)_2 \cdot 4H_2O$	6	0.4	60 min, RT	[16]
Chitosan	56	$Cd(NO_3)_2$	6.5	0.5	24h, 20 °C	[17]
Chitosan	100	n.a.	4.5	4	12 h, 25 °C	[18]
Poly(acrylamide)–starch Graft Copolymer	415.92	$CdSO_4$	n.a	1.11	5 h, 20 °C	[19]
Biomass xanthates	19.6	$CdCl_2$	6-8	0.20	2h, 20 °C	[20]
Graphene oxide composite (GO-starch)	29.04	n.a.	n.a	2.5	2h, 25 °C	[21]
Dialdehyde phenylhydrazine starch (DASPH)	550.8	n.a.	5.0	-	2h, -	[22]
Crosslinked carboxymethyl starch (CCS)	47	$CdCl_2$	6	50	1h, 25 °C	[23]

Table S6. Sorption capacities for removal of Pb^{2+} compounds from aqueous solutions with different sorbent materials and adsorbent doses (a.d.). The obtained sorption capacities from this work were achieved in the batch adsorption experiments.

Material	Sorption Capacity q (mg/g)	Salt	Experimental Conditions			Ref.
			pH_0	a.d. (g/L)	t, T	
Oxidized potato starch	21.6	$PbSO_4$	5.6	0.2	2 h, 25 °C	This work
Oxidized corn starch	18.4	$PbSO_4$	5.6	0.2	2 h, 25 °C	This work
Native potato starch	3.5	$PbSO_4$	5.6	2	2 h, 25 °C	This work
Aspergillus niger	4.7	$Pb(NO_3)_2$	6.01	5.22	24 h, 30 °C	[12]
Anthranilic acid/*o*-toluidine/formaldehyde (AOTF)	30.31	n.a.	6.0	1	24 h, 21 °C	[24]
Typha domingensis leaf powder	0.65	n.a.	2.5	10	120 min, 25 °C	[4]
Carbon prepared from apricot stone (ASAC)	22.85	$Pb(NO_3)_2$	6	2	48 h, 25 °C	[14]
Sporopollenin	8.52	$Pb(NO_3)_2$	6	16.67	60 min, 20 °C	[15]
L. japonica algae	1.68	$Pb(NO_3)_2$	4.5	1	30 h, -	[6]
Glutaraldehyde-cross-linked epoxyaminated chitosan (GA-C-ENCS)	150	$Pb(NO_3)_2$	5.5	2	3h, 20 °C	[25]
CS/PVA/DNDs	121.3	n.a	6	0.4	24h, 20 °C	[26]
Chitosan-Modified fast pyrolysis BioChar (CMBC)	5.8	$Pb(NO_3)_2$	5	2	24h, 25 °C	[27]
Dithiocarbamate-modified starch (DTC)	80.80	$Pb(NO_3)_2$	4	0.1	12 h, 25 °C	[28]
DTC enzymolysis starch (DTCES)	118.10	$Pb(NO_3)_2$	4	0.1	12 h, 25 °C	[28]
DTC mesoporous starch (DTCMS	261.07	$Pb(NO_3)_2$	4	0.1	12 h, 25 °C	[28]
Crosslinked-amphoteric-starch (CAS 1)	21.01	$Pb(NO_3)_2$	4	0.8	1 h, 20 °C	[29]
CAS 2	62.11	$Pb(NO_3)_2$	4	0.8	1 h, 20 °C	[29]
CAS 3	156.25	$Pb(NO_3)_2$	4	0.8	1 h, 20 °C	[29]
Itaconate starch semiester (SI)	506.44	$Pb(NO_3)_2$	-	2	24 h, RT	[30]
Itaconate Starch Diester (DI)	145.03	$Pb(NO_3)_2$	-	2	24 h, RT	[30]
Cationic starch bearing primary amine group	53.4	$PbSO_4$	6	1.25	24 h, -	[31]
Humic acid/starch	176.29	$PbCl_2$	5	1	2.5 h, 25 °C	[32]

composite microspheres (HS-CM)						
Three-dimonsional nanoporous starch based nanomaterial (EDTA/3D-PSN)	238.39	$Pb(NO_3)_2$	-	0.2	12 h, 25 °C	[33]
Fe_2O_3 NPs-Starch	2000	$Pb(NO_3)_2$	6	0.4	60 min, RT	[16]
Biopolymer-modified MNPs	46	$Pb(NO_3)_2$	5.5	2	4h, 25 °C	[34]
Cassava-starch-5-cholоromethyl-8-hydroxyquinoline polymer(CSCMQ)	43.859	$Pb(NO_3)_2$	6	1	2h, 35 °C	[35]
Modified potato starch-magnetic nanoparticles, MPS-MNPs	70	$Pb(NO_3)_2$	5.5	2	2h, 35 °C	[36]
Starch reinforced with TDI-modified birch cellulose	66.66	$Pb(NO_3)_2$	5	4	120 h, 25 °C	[37]
Poly(acrylamide)–starch Graft Copolymer	660	$PbSO_4$	n.a.	1.11	5 h, 20 °C	[19]
Biomass xanthates	27.55	$Pb(NO_3)_2$	6-8	0.20	2h, 20 °C	[20]
Dialdehyde phenylhydrazine starch (DASPH)	290.1	-	5.0	-	2h, -	[22]
Crosslinked carboxymethyl starch (CCS)	80	$Pb(NO_3)_2$	6	50	1h, 25 °C	[23]

3. References

1. Cael, J.J.; Koenig, J.L.; Blackwell, J. Infrared and Raman spectroscopy of carbohydrates. Part VI: Normal coordinate analysis of V-amylose. *Biopolymers* **1975**, *14*, 1885–1903, doi:10.1002/bip.1975.360140909.
2. Cael, S.J.; Koenig, J.L.; Blackwell, J. Infrared and raman spectroscopy of carbohydrates. *Carbohydr. Res.* **1973**, *29*, 123–134, doi:10.1016/S0008-6215(00)82075-3.
3. Kizil, R.; Irudayaraj, J.; Seetharaman, K. Characterization of irradiated starches by using FT-Raman and FTIR spectroscopy. *J. Agric. Food Chem.* **2002**, *50*, 3912–3918, doi:10.1021/jf011652p.
4. Abdel-Ghani, N.T.; Hegazy, A.K.; El-Chaghaby, G.A. Typha domingensis leaf powder for decontamination of aluminium, iron, zinc and lead: Biosorption kinetics and equilibrium modeling. *Int. J. Environ. Sci. Technol.* **2009**, *6*, 243–248, doi:10.1007/BF03327628.
5. Al-Muhtaseb, S.A.; El-Naas, M.H.; Abdallah, S. Removal of aluminum from aqueous solutions by adsorption on date-pit and BDH activated carbons. *J. Hazard. Mater.* **2008**, *158*, 300–307, doi:10.1016/j.jhazmat.2008.01.080.
6. Lee, H.S.; Suh, J.H.; Kim, I.B.; Yoon, T. Effect of aluminum in two-metal biosorption by an algal biosorbent. *Miner. Eng.* **2004**, *17*, 487–493, doi:10.1016/j.mineng.2004.01.002.
7. pour, P.; Takassi, M.; Hamoule, T. Removal of Aluminum from Water and Industrial Waste Water. *Orient. J. Chem* **2014**, *30*, 1365–1369, doi:10.13005/ojc/300356.
8. Choksi, P.M.; Joshi, V.Y. Adsorption kinetic study for the removal of nickel (II) and aluminum (III) from an aqueous solution by natural adsorbents. *Desalination* **2007**, *208*, 216–231, doi:10.1016/j.desal.2006.04.081.
9. Lobo-Recio, M.Á.; Lapolli, F.R.; Belli, T.J.; Folzke, C.T.; Tarpani, R.R.Z. Study of the removal of residual aluminum through the biopolymers carboxymethylcellulose, chitin, and chitosan. *Desalination Water Treat.* **2013**, *51*, 1735–1743, doi:10.1080/19443994.2012.715133.
10. Samadi, N.; Hasanzadeh, R.; Rasad, M. Adsorption isotherms, kinetic, and desorption studies on removal of toxic metal ions from aqueous solutions by polymeric adsorbent. *J. Appl. Polym. Sci.* 2014, n/a-n/a, doi:10.1002/app.41642.
11. Rao, K.S.; Anand, S.; Venkateswarlu, P. Adsorption of Cadmium from Aqueous Solution by Ficus religiosa Leaf Powder and Characterization of Loaded Biosorbent. *Clean Soil Air Water* **2011**, *39*, 384–391, doi:10.1002/clen.201000098.
12. Amini, M.; Younesi, H. Biosorption of Cd(II), Ni(II) and Pb(II) from Aqueous Solution by Dried Biomass of Aspergillus niger: Application of Response Surface Methodology to the Optimization of Process Parameters. *Clean Soil Air Water* **2009**, *37*, 776–786, doi:10.1002/clen.200900090.
13. Thangaraj, V.; Aravamudan, K.; Lingam, R.; Subramanian, S. Individual and simultaneous adsorption of Ni (II), Cd (II), and Zn (II) ions over polyamide resin: Equilibrium, kinetic and thermodynamic studies. *Env. Prog Sustain. Energy* **2019**, *38*, S340–S351, doi:10.1002/ep.13056.
14. Kobya, M.; Demirbas, E.; Senturk, E.; Ince, M. Adsorption of heavy metal ions from aqueous solutions by activated carbon prepared from apricot stone. *Bioresour. Technol.* **2005**, *96*, 1518–1521, doi:10.1016/j.biortech.2004.12.005.
15. Unlü, N.; Ersoz, M. Adsorption characteristics of heavy metal ions onto a low cost biopolymeric sorbent from aqueous solutions. *J. Hazard. Mater.* **2006**, *136*, 272–280, doi:10.1016/j.jhazmat.2005.12.013.
16. Mahmoud, M.E.; Nabil, G.M.; Zaki, M.M.; Saleh, M.M. Starch functionalization of iron oxide by-product from steel industry as a sustainable low cost nanocomposite for removal of divalent toxic metal ions from water. *Int. J. Biol. Macromol.* **2019**, *137*, 455–468, doi:10.1016/j.ijbiomac.2019.06.170.
17. Jha, I.N.; Iyengar, L.; Prabhakara Rao, A.V.S. Removal of Cadmium Using Chitosan. *J. Environ. Eng.* **1988**, 962–974, doi:10.1061/(ASCE)0733-9372(1988)114:4(962).

18. Bamgbose, J.T.; Adewuyi, S.; Bamgbose, O.; Adetoye A. A. Adsorption kinetics of cadmium and lead by chitosan. *Afr. J. Biotechnol.* **2010**, 2560–2565, doi:10.5897/AJB2010.000-3071.
19. Khalil, M.I.; Farag, S. Utilization of some starch derivatives in heavy metal ions removal: National Research Centre, Textile Research Division, Dokki, Egypt. *J. Appl. Polym. Sci.* **1997,** 45–50, doi:10.1002/(SICI)1097-4628(19980705)69:1<45:AID-APP6>3.0.CO;2-M.
20. Li, W.; Liao, X.; Wang, L.; Huang, Z. Adsorption of cadmium and lead in wastewater by four kinds of biomass xanthates. *Water Sci. Technol.* **2019**, *79*, 1222–1230, doi:10.2166/wst.2019.124.
21. Wang, Z.; Zhang, X.; Wu, X.; Yu, J.-G.; Jiang, X.-Y.; Wu, Z.-L.; Hao, X. Soluble starch functionalized graphene oxide as an efficient adsorbent for aqueous removal of Cd(II): The adsorption thermodynamic, kinetics and isotherms. *J. Sol-Gel. Sci. Technol.* **2017**, *82*, 440–449, doi:10.1007/s10971-017-4313-3.
22. Wang, R.; Liu, J.-T.; Li, C.-Y.; Li, R. Removal of transition metal ions from aqueous solution using dialdehyde phenylhydrazine starch as adsorbent. *Water Sci. Technol.* **2014**, *69*, 479–485, doi:10.2166/wst.2013.571.
23. Chen, Y.X.; Zhong, B.H.; Fang, W.M. Adsorption characterization of lead(II) and cadmium(II) on crosslinked carboxymethyl starch. *J. Appl. Polym. Sci.* **2012**, *124*, 5010–5020, doi:10.1002/app.35607.
24. Azarudeen, R.S.; Riswan Ahamed, M.A.; Subha, R.; Burkanudeen, A.R. Heavy and toxic metal ion removal by a novel polymeric ion-exchanger: synthesis, characterization, kinetics and equilibrium studies. *J. Chem. Technol. Biotechnol.* **2015**, *90*, 2170–2179, doi:10.1002/jctb.4528.
25. Rijith, S.; Anirudhan, T.S.; Sumi, V.S.n.; Shripathi, T. Sorptive potential of glutaraldehyde cross-linked epoxyaminated chitosan for the removal of Pb(II) from aqueous media: kinetics and thermodynamic profile. *Desalination Water Treat.* **2016**, *57*, 15083–15097, doi:10.1080/19443994.2015.1079252.
26. Vatanpour, V.; Salehi, E.; Sahebjamee, N.; Ashrafi, M. Novel chitosan/polyvinyl alcohol thin membrane adsorbents modified with detonation nanodiamonds: Preparation, characterization, and adsorption performance. *Arab. J. Chem.* **2020**, *13*, 1731–1740, doi:10.1016/j.arabjc.2018.01.010.
27. Bombuwala Dewage, N.; Fowler, R.E.; Pittman, C.U.; Mohan, D.; Mlsna, T. Lead (Pb 2+) sorptive removal using chitosan-modified biochar: batch and fixed-bed studies. *RSC Adv.* **2018**, *8*, 25368–25377, doi:10.1039/C8RA04600J.
28. Xiang, B.; Fan, W.; Yi, X.; Wang, Z.; Gao, F.; Li, Y.; Gu, H. Dithiocarbamate-modified starch derivatives with high heavy metal adsorption performance. *Carbohydr. Polym.* **2016**, *136*, 30–37, doi:10.1016/j.carbpol.2015.08.065.
29. Xu, S.-M.; Feng, S.; Peng, G.; Wang, J.-D.; Yushan, A. Removal of Pb (II) by crosslinked amphoteric starch containing the carboxymethyl group. *Carbohydr. Polym.* **2005**, *60*, 301–305, doi:10.1016/j.carbpol.2005.01.018.
30. Soto, D.; Urdaneta, J.; Pernía, K.; León, O.; Muñoz-Bonilla, A.; Fernandez-García, M. Removal of heavy metal ions in water by starch esters. *Starch Stärke* **2016**, *68*, 37–46, doi:10.1002/star.201500155.
31. Rupf. Preparation of Some Cationic Starches Using the Dry Process.
32. Su, X.; Hu, J.; Zhang, J.; Liu, H.; Yan, C.; Xu, J.; Ma, Y.; Song, J. Investigating the adsorption behavior and mechanisms of insoluble Humic acid/starch composite microspheres for metal ions from water. *Colloids Surf. A Physicochem. Eng. Asp.* **2021**, *610*, 125672, doi:10.1016/j.colsurfa.2020.125672.
33. Fang, Y.; Lv, X.; Xu, X.; Zhu, J.; Liu, P.; Guo, L.; Yuan, C.; Cui, B. Three-dimensional nanoporous starch-based material for fast and highly efficient removal of heavy metal ions from wastewater. *Int. J. Biol. Macromol.* **2020**, *164*, 415–426, doi:10.1016/j.ijbiomac.2020.07.017.
34. Perez, T.; Pasquini, D.; Faria Lima, A. de; Rosa, E.V.; Sousa, M.H.; Cerqueira, D.A.; Morais, L.C. de. Efficient removal of lead ions from water by magnetic nanosorbents based on manganese

ferrite nanoparticles capped with thin layers of modified biopolymers. J. *Environ. Chem. Eng.* **2019**, *7*, 102892, doi:10.1016/j.jece.2019.102892.

35. Shah, P.U.; Raval, N.P.; Vekariya, M.; Wadhwani, P.M.; Shah, N.K. Adsorption of lead (II) ions onto novel cassava starch 5-cholоromethyl-8-hydroxyquinoline polymer from an aqueous medium. *Water Sci. Technol.* **2016**, *74*, 943–956, doi:10.2166/wst.2016.284.
36. Abdul-Raheim, A.-R.M. Low Cost Biosorbents Based On Modified Starch Iron Oxide Nanocomposites For Selective Removal Of Some Heavy Metals From Aqueous Solutions. *AML* **2016**, *7*, 402–409, doi:10.5185/amlett.2016.6061.
37. Anghel, N.; Marius, N.; Spiridon, I. Heavy metal adsorption ability of a new composite material based on starch strengthened with chemically modified cellulose. *Polym. Adv. Technol.* **2019**, *30*, 1453–1460, doi:10.1002/pat.4577.